RESEARCH ARTICLE

Optimal Distributed Generation Placement in Radial Distribution Networks Using Enhanced Search Group Algorithm

TRUONG HOANG BAO HUY[1], **DIEU NGOC VO**[2,3], **KHOA HOANG TRUONG**[3,4],
AND THANH VAN TRAN[5]

[1]Department of Future Convergence Technology, Soonchunhyang University, Asan-si, Chuncheongnam-do 31538, South Korea
[2]Department of Power Systems, Ho Chi Minh City University of Technology (HCMUT), Ho Chi Minh City 700000, Vietnam
[3]Vietnam National University Ho Chi Minh City, Linh Trung Ward, Thu Duc, Ho Chi Minh City 700000, Vietnam
[4]Department of Power Delivery, Ho Chi Minh City University of Technology (HCMUT), Ho Chi Minh City 700000, Vietnam
[5]Institute of Engineering and Technology, Thu Dau Mot University, Thu Dau Mot City, Binh Duong 75109, Vietnam

Corresponding author: Thanh Van Tran (thanhtv@tdmu.edu.vn)

ABSTRACT The aim of this research is to define the placement of distributed generations (DGs) in radial distribution networks (RDNs) using a meta-heuristic method called the Enhanced Search Group Algorithm (ESGA). This algorithm is an upgraded version of the conventional SGA that incorporates the Chaotic Local Search (CLS) approach to improve global exploration ability. The purposes of the optimal DG placement (ODGP) problem are to decrease active power losses, increase voltage stability, and boost the voltage profile of RDNs. The study applied the ESGA to optimize the placement and size of DGs, considering two cases of power factors (unity and optimal) in 33, 69, and 118-bus RDNs. Based on the optimal results, employing optimal power factors in operating DGs pointedly enhances the performance of RDNs by decreasing power loss, reducing voltage deviation, and increasing voltage stability. The ESGA method outperforms other approaches regarding solution quality, indicating its effectiveness in resolving ODGP problems, particularly for large-scale and complex networks.

INDEX TERMS Search group algorithm, distributed generation, optimal power factor, power loss, voltage profile, voltage stability.

I. INTRODUCTION

The demand for electricity on a global scale is expected to increase significantly in the next few decades [1]. An energy report from BloombergNEF predicts that the demand for electricity worldwide will rise from 25 billion MWh in 2017 to approximately 38.7 billion MWh in 2050, representing a 57% increase [2]. Traditionally, meeting this demand would involve expanding existing power systems and constructing new centralized power plants, which incurs substantial investment and operational expenses. Additionally, electricity generation from fossil fuels or nuclear power plants can have adverse environmental impacts. Integration

of Distributed Generation (DG) in power grids is considered a potential solution. DG is a more economical option since it involves the production of electricity on a smaller scale as opposed to centralized power plants, and the technology used in DG is primarily from renewable energies (e.g., wind, solar, geothermal, hydrogen, biomass, and ocean), leading to environmental benefits [3]. Appropriate allocation of DGs connected to radial distribution networks (RDNs) can lead to the reduction of power loss and enhancement of system voltage. Moreover, integrating DG can delay network reinforcement and reduce the transmission lines' capacity [3]. Nevertheless, the misallocation of DGs can lead to decreased system stability, voltage fluctuations, and high power losses [4]. Therefore, it is crucial to identify the appropriate sizes and locations of DGs to ensure maximum

The associate editor coordinating the review of this manuscript and approving it for publication was Lei Chen.

technical, economic, and environmental advantages in the planning of RDNs.

Over the past decade, researchers have shown considerable interest in the optimal placement of DGs (ODGP) in RDNs, due to the significant benefits of DG. Analytical methods have been proposed in numerous studies to resolve ODGP problems. A study introduced an analytical method in [5] to find the optimum sizes and positions of DGs with the objective of reducing active power losses. The method includes an analytical expression and an effective methodology that both use the exact loss formula. The reference in [6] improved the analytical method proposed in [5] by developing a comprehensive formula. This new formula was designed to find the op optimum sizes and positions of various kinds of DGs. A two-phase method for the ODGP problems was introduced in [7]. The first phase used the voltage stability state and loss sensitivity of nodes to determine an appropriate DG position, while the analytical expressions were utilized to estimate the optimal sizes of the DGs in the second phase. Although analytical methods have advantages such as short computational time and easy implementation, they may face challenges when dealing with complex problems that involve many DGs, diverse forms of DGs, or multiple objective functions. Additionally, analytical approaches could struggle to handle large-scale problems.

For solving ODGP problems, artificial intelligence-based methods have also been explored as an alternative approach. For instance, in [8], researchers used a Genetic Algorithm (GA) that considered uncertainties in renewable DG and load demand. This method was used to assess various costs associated with system upgrades, energy loss, and interruption. Researchers in [9] proposed an approach to address the multi-objective ODGP problem using a cloud theory adapted GA (AGA). This approach considers various indexes such as power losses, line load capability, voltage stability, and voltage profile, voltage stability. A judgment matrix was used to define the weight for each index. The ODGP issue in RDNs has been tackled using adaptive GA (AGA) with an on-load tap changer (OLTC) in [10], where two AGA variants were proposed to minimize a combined objective function related to voltage deviation and active power losses. To address the ODGP problem in RDNs, Particle Swarm Optimization (PSO) is a widely used artificial intelligence technique. In [11], a multi-objective function was formulated by considering various objectives, including short-circuit level, the capacity of conductors, active power loss, and reactive power loss of the system. The PSO method was applied to solve this problem using different load models. In [12], PSO was utilized to identify the appropriate placement of various DGs to decrease the active power losses of the system, utilizing the precise loss formulation. Different variants of the PSO technique have been employed, as demonstrated in several studies: multi-objective evolutionary PSO (MEPSO) [13], binary PSO [14], and discrete PSO [15]. These methods have

shown success in finding optimal solutions for the ODGP problem. To summarize, both GA and PSO are artificial intelligence techniques that can be applied to solve the ODGP problem. However, each method has its limitations. GA can be time-consuming and may not find a global solution. On the other hand, PSO has better global search ability and its ability to define the global solution for large-scale problems is not guaranteed. Additionally, both methods require careful tuning of their parameters to obtain good solutions [16].

There are various other AI-based methods that have been utilized to optimize the ODGP problems in RDNs. The authors in [17] used the artificial bee colony (ABC) approach for defining the optimum positions and capacities of DGs with the aim of curtailing the active power losses. Ref. [18] introduced a method based on Cuckoo Search (CS) to solve the ODGP problems, which aims to enhance the voltage profile and decrease power losses in RDNs. The ODGP in RDNs was investigated using the Backtracking Search Optimization Algorithm (BSOA) in [19]. A combined objective function of voltage profile and power loss was formulated based on weighted coefficients. Ref. [20] used Ant Lion Optimizer (ALO) to identify optimal settings of renewable DGs, wherein the Loss Sensitivity Factors (LSFs) approach was used to identify potential nodes. The ODGP problem in RDNs was tackled in [21] using the Krill Herd Algorithm (KHA) method, which aimed to optimize energy losses and system power losses. The authors in [22] introduced a capuchin search algorithm (CapSA) to determine the optimal sizes and locations of biomass DGs in distribution systems, wherein they also conducted sensitivity analyses concerning various numbers of DGs. In [23], presented the chimp optimizer (CO) was presented as a solution for the ODGP on 33-, 69-, and 119-bus systems. That study considered two modes of DGs, namely unity and non-unity power factors. In [24], ODGP problem was solved by an improved wild horse optimizer (IWHO) to enhance the system reliability, improve the voltage profile, and reduce operational losses. Several methods have also recently been developed to solve the ODGP problem, such as the modified gravitational search algorithm with expert experience (MGSA-EE) [25], artificial hummingbird algorithm (AHA) [26], adaptive equilibrium optimizer (AEO) [27], crystal structure algorithm (CrSA), war strategy optimizer (WSO), and average and subtraction-based optimizer (ASBO) [28]. For finding an optimal or near-optimal solution, artificial intelligence-based approaches are commonly used. However, some of these methods may encounter local optimization and demand a high computational cost for complicated problems.

Hybrid methods have been created to address ODGP problems. These hybrid methods combine the strengths of individual methods to enhance either the convergence speed or accuracy of the hybrid algorithm. Ref. [29] introduced a combination of PSO and GA techniques to optimize the locations and power outputs of DGs in RDNs. DG locations were defined using GA while DG capacities were optimized

using PSO. The primary objective was to concurrently enhance voltage stability, reduce active power loss, and boost voltage regulation in RDNs. The authors in Ref. [29] also suggested an alternative hybrid approach called GA/IWD, as described in [30], that combines the GA and Intelligent Water Drops (IWD) algorithms to tackle the identical problem addressed in their earlier study. Similarly, a hybrid approach called AM-PSO was developed to address the ODGP problem, as detailed in [31]. This approach combines an analytical method for evaluating the capacities of DG units with PSO for locating their optimal positions, thereby achieving minimal power loss in the network. Ref. [32] introduced an approach named EA-OPF for addressing the ODGP issue with the goal of minimizing power losses. This technique combines the optimal power flow (OPF) method and an effective analytical (EA) approach. Initially, the EA method was employed to obtain the optimal locations of DGs. Afterward, OPF was utilized to calculate the optimum capacities of the DGs at those specific locations. While hybrid approaches often yield superior solutions compared to standalone methods, they can pose challenges in terms of implementation and computational resources due to their complex structures and numerous control parameters.

In past studies, several methods were suggested to tackle ODGP problems with similar objective functions as in [29], [30], including Stochastic Fractal Search (SFS) [33], Chaotic Symbiotic Organism Search (CSOS) [34], Quasi-Oppositional Swine Influenza Model-Based Optimizer with Quarantine (QOSIMBO-Q) [35], and Quasi-Oppositional Teaching Learning Based Optimizer (QOTLBO) [36]. The studies [34] and [36] focused on the implementation of DG units with a unity power factor. On the other hand, optimal DG power factors and large-scale systems have not been considered for the ODGP problem in [35]. The previous studies mentioned have not adequately considered the impact of varying DG power factors on the performance of the RDNs. As per IEEE 1547 standard [37], DGs are capable of operating at any power factor. Hence, it is required to study various power factors of DGs in the ODGP problem. Although a variety of metaheuristic algorithms have been applied to the ODGP problem, they encounter problems with convergence speed and may become trapped in local optima. Additionally, certain studies focused solely on a single small-scale system, which insufficiently validates the reliability of the proposed approach. Moreover, the DGs integration still has certain limitations, necessitating additional research. As the ODGP problem can be more complicated when considering the DG power factor, developing an algorithm is necessary to effectively resolve the ODGP problem.

The goal of this research work is to solve the ODGP problem to reduce active power losses, minimize voltage deviation, and maximize the voltage stability of RDNs. To address the ODGP framework, the study introduces a novel meta-heuristic method called the Enhanced Search Group Algorithm (ESGA). The conventional SGA is combined with a Chaotic Local Search (CLS) approach to progress its global exploration capability and convergence speed. The study employs the proposed ESGA method to identify optimal locations and sizes of DG units in the 33, 69, and 118-bus RDNs under various objective function scenarios. The contributions of the study are given below:

- The study suggests an improved algorithm (ESGA) to tackle the ODGP framework with a single objective function of active power loss reduction, while also optimizing multiple objective functions of active power loss, voltage stability, and voltage profile simultaneously.
- The study evaluates the performance of the suggested ESGA on three different RDNs: the 33-bus, 69-bus, and 118-bus networks. The results attained by ESGA are compared against those attained by the conventional SGA and other previously published studies. The comparisons demonstrate that ESGA outperforms the other methods and provides a superior solution.
- The study investigates the influence of DG power factors on RDNs. The findings show that operating the optimal DGs power factors leads to a substantial enhancement in RDNs performance, including reducing power loss, minimizing voltage deviation, and maximizing voltage stability.
- The ODGP problem is investigated in a scenario that accounts for daily variable load and DG uncertainty, wherein the objective function is to minimize daily energy loss for a representative day.

Section II outlines the ODGP formulation. Section III introduces a detailed presentation of the suggested ESGA. Section IV explains the ESGA employment to the ODGP optimization. The simulation outcomes are presented in Section V, and the study concludes with a summary of findings in Section VI.

II. PROBLEM FORMULATION

The goal of the ODGP is to find the best positions and capacities for DGs in an RDN, in order to decrease active power loss and voltage deviation, while also increasing the voltage stability index. All constraints related to the system operation must be met.

A. ACTIVE POWER LOSS

The formula of the active power loss (P_L) in an RDN is as follows:

$$P_L = \sum_{l=1}^{N_L} R_l I_l^2 \tag{1}$$

where N_L denotes the number of branches in RDN, I_l denotes the current passing through the lth branch, and R_l denotes the resistance of the lth branch.

B. VOLTAGE DEVIATION (VD)

Voltage profile improvement aims to minimize the voltage deviation (VD) of all load buses from 1.0 p.u., which can be
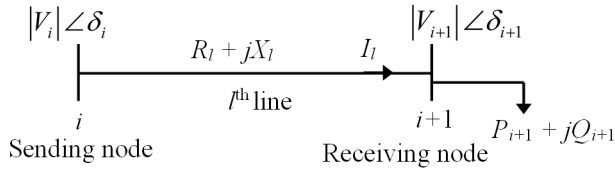
FIGURE 1. A single line in a distribution network.

described in the following equation:

$$VD = \sum_{i=1}^{N_B} (V_i - 1.0)^2 \tag{2}$$

where N_B denotes the number of buses in an RDN, and V_i is the voltage magnitude at the ith bus.

C. VOLTAGE STABILITY INDEX (VSI)

The VSI at the $(i + 1)^{th}$ bus is determined by [38]:

$$VSI_{i+1} = |V_i|^4 - 4(P_{i+1}X_l - Q_{i+1}R_l) \\ - 4(P_{i+1}R_l + Q_{i+1}X_l)|V_i|^2 \tag{3}$$

where the power of P_{i+1} and Q_{i+1}, as shown in Fig. 1, is calculated as follows [31]:

$$P_{i+1} - jQ_{i+1} = I_l \times V_{i+1} \tag{4}$$

where:

$$I_l = \frac{V_i - V_{i+1}}{R_l + jX_l} \tag{5}$$

where X_l denotes the reactance of the lth branch.

D. OBJECTIVE FUNCTIONS

The ODGP problem under study is represented as a mathematical model that includes both single-objective and multi-objective problems:

1) SINGLE OBJECTIVE FUNCTION

In the case of the single objective, only active power loss minimization is considered in the ODGP as follows:

$$FF = \min(P_L) \tag{6}$$

2) MULTI-OBJECTIVE FUNCTION

In this study, three objective functions, including power loss, voltage deviation, and voltage stability index are optimized simultaneously. To this end, the weighted metric method is applied to deal with multi-objective problems. This method converts a multi-objective function into a single-objective function by assigning weighting factors to the objective functions. Accordingly, the three functions P_L, VD, and VSI^{-1} are merged as follows [29]:

$$FF = \min\left(\frac{P_L}{P_{L,base}} + \omega_1 \frac{VD}{VD_{base}} + \omega_2 \frac{VSI^{-1}}{VSI_{base}^{-1}}\right) \tag{7}$$

where ω_1 and ω_2 are weighting factors, chosen as 0.6 and 0.35, respectively. The values of the weighting factors in Eq. (7) are kept the same values in the study [29] for fair result comparisons. Furthermore, the objective functions in Eq. (7) are normalized by dividing by their corresponding base.

E. SYSTEM CONSTRAINTS

The equality and inequality constraints of the ODGP problem are described below:

1) POWER BALANCE

In an RDN, the total generation including powers from the slack bus and power outputs of DG units must equal power load demands plus system power losses. The power balance equations of active and reactive powers in an RDN are described below:

$$P_{SS} + \sum_{n=1}^{N_{DG}} P_{DG,n} = \sum_{i=1}^{N_B} P_{D,i} + \sum_{l=1}^{N_L} P_{L,l} \tag{8}$$

$$Q_{SS} + \sum_{n=1}^{N_{DG}} Q_{DG,n} = \sum_{i=1}^{N_B} Q_{D,i} + \sum_{l=1}^{N_L} Q_{L,l} \tag{9}$$

where N_{DG} is the number of DG units; P_{SS} and Q_{SS} are powers injected from the reference bus; $P_{DG,n}$ and $Q_{DG,n}$ represent power generated from the nth DG unit; $P_{D,i}$ and $Q_{D,i}$ represent power load demands by the ith bus; $P_{L,l}$ and $Q_{L,l}$ represent power losses in the lth branch.

2) VOLTAGE CONSTRAINT

The voltage magnitude at each bus is restricted as follows:

$$V_{\min,i} \le V_i \le V_{\max,i}; \quad i = 1, \ldots, N_B \tag{10}$$

in which $V_{\min,i}$ and $V_{\max,i}$ represent the voltage limits at the ith bus, respectively.

3) THERMAL CONSTRAINT

The current flowing through a line ought not to violate its maximum capacity:

$$|I_l| \le |I_{\max,l}|; \quad l = 1, \ldots, N_L \tag{11}$$

in which $I_{\max,l}$ represents the maximum loading of the lth branch.

4) DG GENERATION CONSTRAINT

The power generated from each DG unit is limited by the following equations:

$$P_{DG\min,n} \le P_{DG,n} \le P_{DG\max,n}; \quad n = 1, \ldots, N_{DG} \tag{12}$$

where $P_{DG\min,n}$ and $P_{DG\max,n}$ represent the power output limits of nth DG unit.

The reactive power $Q_{DG,n}$ and apparent power $S_{DG,n}$ from DGs can be defined as follows:

$$Q_{DG,n} = P_{DG,n} \cdot \tan(\cos^{-1}(pf_{DG,n})) \tag{13}$$

$$S_{DG,n} = \sqrt{P_{DG,n}^2 + Q_{DG,n}^2} \tag{14}$$

where $pf_{DG,n}$ represents the power factor of nth DG unit.

5) DG POWER FACTOR CONSTRAINT
DG power factors are limited as follows:

$$pf_{DG\min,n} \leq pf_{DG,n} \leq pf_{DG\max,n}; \quad n = 1, \ldots, N_{DG} \quad (15)$$

where $pf_{DG\min,n}$ and $pf_{DG\max,n}$ represent the power factor limits of nth DG unit.

6) DG PENETRATION CONSTRAINT
The total power generated from each DG ought to be less than or equal to the total power load demand:

$$\sum_{n=1}^{N_{DG}} P_{DG,n} \leq \sum_{i=1}^{N_B} P_{D,i} \quad (16)$$

$$\sum_{n=1}^{N_{DG}} S_{DG,n} \leq \sum_{i=1}^{N_B} S_{D,i} \quad (17)$$

where $S_{D,i}$ represents the apparent power load demand at the ith bus.

III. ENHANCED SEARCH GROUP ALGORITHM
The ESGA is an upgraded version of the SGA that incorporates a chaotic local search (CLS) technique. With the integration of this technique, the ESGA algorithm can effectively exploit the area around the best solution, resulting in better optimization results. By implementing the CLS method, the ESGA can converge to the optimal solution more quickly and generate higher-quality solutions for optimization problems.

A. SGA
SGA is an optimization algorithm introduced in [39], which aims to achieve an optimal balance between exploring and exploiting the design domain. In the beginning, it explores the domain to locate promising areas, and then in subsequent iterations, it exploits those areas to search for the best solution. The optimization process of the SGA is regulated by a parameter called the perturbation constant (α), while the mutation phase generates replacement solutions for the current search group, wherein the search group comprises a group of individuals who create these new solutions.

Firstly, SGA initializes a population of n_p solutions from the search domain as follows:

$$X_i = X_{\min} + rand(0, 1)(X_{\max} - X_{\min}); \quad i = 1, \ldots, n_p \quad (18)$$

where n_p is the population size, X_i denotes the ith solution vector in the initial population, $rand(0, 1)$ denotes a random number between 0 and 1, and $X_{\min}$ and $X_{\max}$ denote the boundaries for each dimension of the problem, respectively.

Afterward, the entire population is evaluated, and a standard tournament selection process is used to choose n_g individuals from population **P**, which forms a search group **R**. The search group is then subjected to mutations during each iteration to improve the global searchability of the SGA algorithm. In each mutation step, a number of new individuals are created to replace the n_{mut} members of the search group, as described below:

$$x_{j,mut} = E[R_{:,j}] + t\epsilon\sigma[R_{:,j}]; \quad j = 1, \ldots, D \quad (19)$$

The mutation process involves modifying the jth variable of an individual, denoted as $x_{j,mut}$, using the mean value operator (E), standard deviation operator (σ), and a random variable (ϵ). The parameter t determines the degree to which new individuals are created, while $R_{:,j}$ represents the jth column of the search group matrix, and D is the number of design variables. The probability of replacing a member of the search group is determined based on the rank of the search group, which is calculated using inverse tournament selection.

After the search group is created and mutated, each member of the search group produces a family as follows:

$$x_{j,new} = R_{i,j} + \alpha\epsilon; \quad j = 1, \ldots, D \quad (20)$$

In this process, the perturbation size is controlled by the parameter α. As the optimization process progresses, the perturbation decreases with each iteration. The value of α is updated using a parameter b as follows:

$$\alpha^{G+1} = b\alpha^G \quad (21)$$

For the global stage, the best member from each family is selected to create the new search group. However, in the local stage, the selection process is adjusted, and the best n_g individuals from all families form a new search group to exploit the region around the current best design.

B. THE PROPOSED ESGA
To improve the searchability and avoid getting stuck in the local optimization of the proposed method, the original SGA is combined with the CLS approach. The ESGA consists of two optimization phases. For the first phase, the SGA technique is used to define the best solutions in the search space. In the second phase, the CLS approach exploits the nearby search space of current search group members to generate better solutions.

For each search group member, a new solution may be generated using CLS in the following equation [40]:

$$X_{i,k}^{new} = X_{i,k} + (Z_k - 0.5) \times (X_{m,k} - X_{n,k}) \quad (22)$$

where $X_{i,k}$ and $X_{i,k}^{new}$ represent the positions of the ith current search group member and new solution created from CLS at k^{th} iteration; $X_{m,k}$ and $X_{n,k}$ denote two random solutions selected from the current search group. The new solution $X_{i,k}^{new}$ will replace the current search group member $X_{i,k}$ in the current search group if its fitness function value is fitter than the current search group member.

In (22), Z_k is a variable of chaotic sequence at the kth iteration, which is created using the logistic map as follows [41]:

$$Z_{k+1} = \mu \times Z_k \times (1 - Z_k) \quad (23)$$

in which $Z_0 = rand(0, 1)$, $Z_k \in (0, 1)$ $\forall \{0, 1, 2, \ldots\}$ and $\mu \in (0, 4]$. The CLS is performed until the maximum iterations of CLS (K) are reached. A pseudocode of the ESGA is outlined in Algorithm 1.

Algorithm 1 Pseudocode of ESGA

Input: n_p, n_g, n_{mut}, α, $G^{\max}$, K
Output: Otimal solution $x^* = R_{1,:}$
1 / * **Step 1: Initialization** * /
2 $x_1, x_2, \ldots, x_{n_p} = $ initialization()
3 **for** $i \leftarrow 1$ to n_p **do**
4 $\quad OF_i = $ fobj (x_i)
5 **end**
6 Sort all individuals of population **P**
7 / **Step 2: Initial search group selection** */
8 Create an initial search group R^G by selecting n_g individuals
$\quad$ from population **P**
9 **for** $G \leftarrow 1$ to $G^{\max}$ **do**
10 $\quad$ /* **Step 3: Mutation of the search group** */
11 $\quad$ index = reverse_tournament ()
12 $\quad$ **for** $j \leftarrow 1$ *to* n_{mut} **do**
13 $\quad\quad$ $x_{new} = $ mutation $\left(R_{index(j)}\right)$
14 $\quad$ **end**
15 $\quad$ / * **Step 4: Generation of the families** */
16 $\quad$ **for** $j \leftarrow 1$ to n_g **do**
17 $\quad\quad$ $F_i = $ family_generation (R_i)
18 $\quad$ **end**
19 $\quad$ / * **Step 5: Selection of the new group** * /
20 $\quad$ % Global phase %
21 $\quad$ Sort each family
22 $\quad$ Form search group R^{G+1} by selecting the best member
$\quad\quad$ of each family
23 $\quad$ % Local phase%
24 $\quad$ Sort members in all families
25 $\quad$ Form search group R^{G+1} by selecting the best n_g
$\quad\quad$ members among all families
26 $\quad$ / * **Step 6: Chaotic local search** * /
27 $\quad$ **for** $i \leftarrow 1$ *to* n_g **do**
28 $\quad\quad$ $X_i = R_i$
29 $\quad\quad$ $Z_0 = rand(0, 1)$
30 $\quad\quad$ **for** $k \leftarrow 1$ *to* K **do**
31 $\quad\quad\quad$ $X_{i,k}^{new} = X_{i,k} + (Z_k - 0.5) \times \left(X_{m,k} - X_{n,k}\right)$
32 $\quad\quad\quad$ **if** $OF\left(X_{i,k}^{new}\right) > OF\left(X_{i,k}\right)$ **then**
33 $\quad\quad\quad\quad$ $X_{i,k} = X_{i,k}^{new}$
34 $\quad\quad\quad$ **end**
35 $\quad\quad\quad$ $Z_{k+1} = \mu \times Z_k \times (1 - Z_k)$
36 $\quad\quad$ **end**
37 $\quad\quad$ $R_i = X_i$
38 $\quad$ **end**
39 **end**

IV. APPLICATION OF ESGA TO ODGP PROBLEM

This study applies the developed ESGA for the ODGP problem with the following two scenarios:

- Scenario I: Minimizing P_L objective.
- Scenario II: Simultaneously optimizing three objectives including P_L, VD, and VSI.

Each scenario is analyzed with regard to the operation of DG units in various cases including:

- Case 1: DGs are operated with a unity power factor.
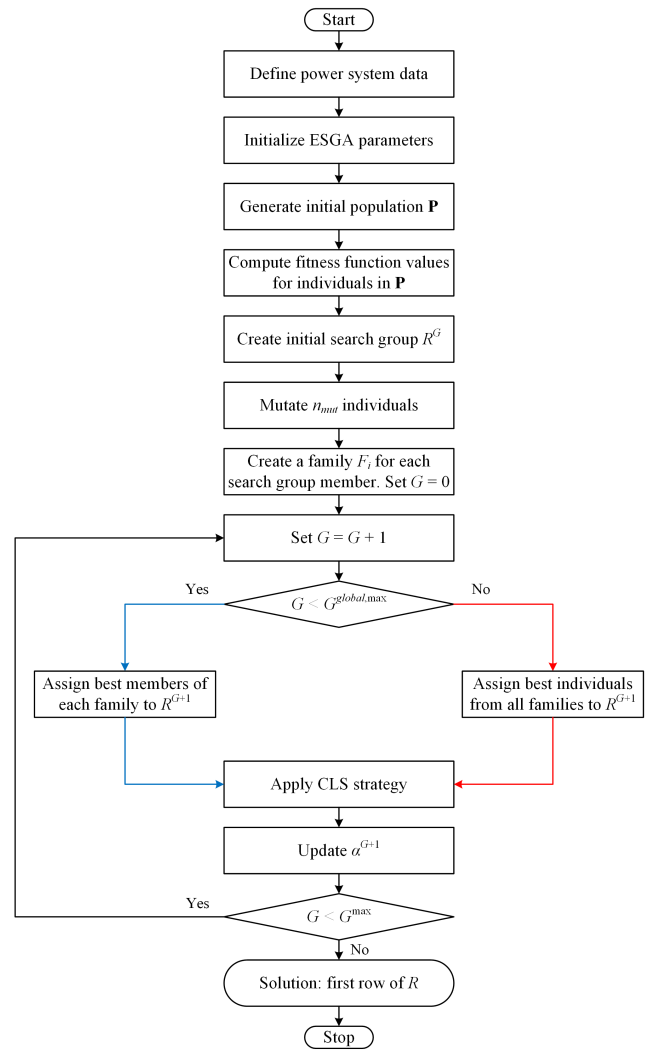- Case 2: DGs are operated with an optimal power factor.

FIGURE 2. Flowchart of ESGA for ODGP problem.

A. POPULATION INITIALIZATION

The initial population in the ESGA is denoted by $X = [X_1, .., X_{n_p}]^T$. Each row of the matrix corresponds to a solution candidate, denoted as $X_i(i = 1, \ldots, n_p)$. For the ODGP problem, the solution vector for Cases 1 and 2 is represented in (24) and (25), respectively, which are given as follows:

$$X_i = [l_{DG,1}, \ldots, l_{DG,N_{DG}}, P_{DG,1}, \ldots, P_{DG,N_{DG}}] \quad (24)$$

$$X_i = [l_{DG,1}, \ldots, l_{DG,N_{DG}}, P_{DG,1}, \ldots, P_{DG,N_{DG}},$$
$$pf_{DG,1}, \ldots, pf_{DG,N_{DG}}] \quad (25)$$

For individuals of ESGA, the solution variables are assigned random values within their respective boundaries during the initialization process as follows:

$$l_{DG,n} = round[l_{DG,\min} + (l_{DG,\max} - l_{DG,\min})$$
$$\times rand(0, 1)] \quad (26)$$

$$P_{DG,n} = P_{DG,\min} + (P_{DG,\max} - P_{DG,\min}) \times rand(0, 1), \quad (27)$$

$$pf_{DG,n} = pf_{DG,\min} + (pf_{DG,\max} - pf_{DG,\min}) \times rand(0, 1)$$
$$(28)$$

where $l_{DG,n}$ is the locations of DG to be installed.

B. FITNESS FUNCTION

Each individual in the population is evaluated using the fitness function presented below:

$$FF_T = FF_m + K_p \sum_{i=1}^{N_B} (V_i - V_i^{\lim})^2 + K_q \sum_{l=1}^{N_L} (I_l - I_l^{\lim})^2$$
$$+ K_v (PE_{DG} - PE_{DG}^{\lim})^2 \qquad (29)$$

The coefficients K_p, K_q, and K_v represent penalties associated with the bus voltage, line current capacity, and DG penetration, respectively, which are set at high values (10^3). As shown in (29), the objective functions correspond to $m = 1$ or 2 depending on the specific scenario being analyzed.

The power flow problem is solved using Matpower 6.0 [42] to calculate the fitness value of each solution in this study. To address constraint violations, a repairing approach is employed in which the variables (i.e., bus voltage, current, and DG penetration) are relocated to their upper or lower bounds as follows:

$$x^{\lim} = \begin{cases} x_{\max} & \text{if} \quad x > x_{\max} \\ x_{\min} & \text{if} \quad x < x_{\min} \\ x & \text{otherwise} \end{cases} \qquad (30)$$

in which x denotes the values of V_i, I_l, and PE_{DG}; $x_{\lim}$ denotes the limits of V_i, I_l, and PE_{DG}.

C. APPLICATION OF ESGA TO THE ODGP PROBLEM

The steps involved in applying the ESGA to solve the ODGP problem are depicted in Fig. 2 and are outlined as follows:

1) Define power system data for the ODGP problem, objective functions to be considered, boundaries for control variables, and set of equality and inequality constraints;
2) Set ESGA parameters: $n_p, n_g, n_{mut}, \alpha, K$, and $G^{\max}$;
3) Initialize randomly a population as described in IV-A;
4) Compute the fitness function value for all individuals in the initial population using (29);
5) Generate an initial search group R^G by selecting n_g best solutions from **P**. Set $G = 0$;
6) Set $G = G + 1$;
7) Mutate n_{mut} individuals according to (19);
8) Each search group member creates a family (F_i) using (20);
9) Select the new search group as follows:
   - Global phase: search group R^{G+1} is formed by selecting the best solution of each family;
   - Local phase: search group R^{G+1} is formed by selecting the best n_g solutions from all families;
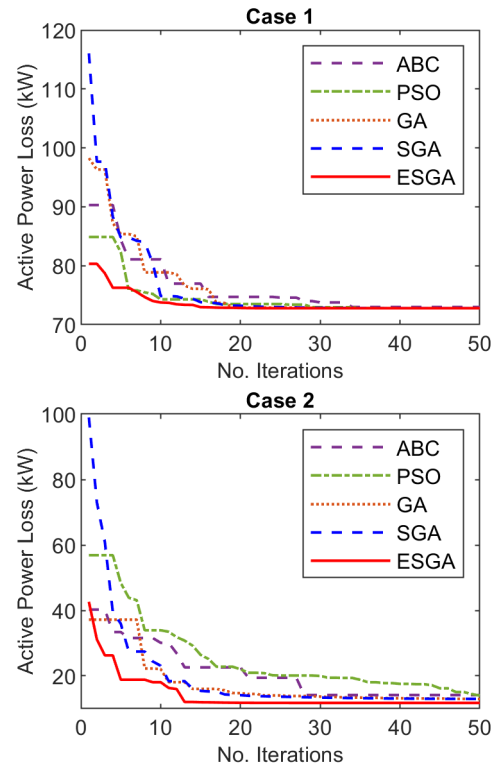10) Apply the CLS strategy to achieve better search group members;

FIGURE 3. Convergence characteristics of ESGA and other methods for Scenario I of 33-bus RDN.

11) Updating α^{G+1} using (21);
12) If $G < G^{\max}$, back to Step 6; otherwise, stop the optimization process.

V. RESULTS

The effectiveness of the proposed ESGA is demonstrated by testing it on 33-bus, 69-bus, and 118-bus RDNs across two scenarios. Each scenario is run through 30 independent trials to obtain the best solution. The control parameters for the ESGA are set as follows: $n_p = 20$, $n_g = 4$, $n_{mut} = 1$ (for 33-bus and 69-bus), $n_p = 100$, $n_g = 20$, $n_{mut} = 2$ (for 118-bus), $\alpha = 2$, and $K = 10$. The value of $G^{\max}$ is selected based on the complication of the test system being solved. In order to compare results, the original SGA and other well-known optimization algorithms, including PSO, GA, and ABC are also implemented to solve the ODGP problem. These methods also use the same population size and the maximum number of iterations as ESGA for the same test system.

A. 33-BUS RDN

Firstly, the 33-bus RDN [43] is used to test the ESGA. The ESGA performs with a maximum iteration $(G^{\max})$ of 50. The active power loss, VD, and VSI^{-1} values are 210.9983 kW, 0.1338 p.u., and 1.4989 p.u, respectively, when no DGs are installed. The test assumes the installation of three DG units.

1) SCENARIO I

In this scenario, the ODGP problem is determined using ESGA to achieve the objective of reducing power loss. In two

TABLE 1. Simulation results of different approaches for Scenario I of 33-bus RDN.

Approaches	Bus	S_{DG}(MVA) / pf	P_L (kW)/ (PLR)	VD (p.u.)	VSI^{-1} (p.u.)	Min VSI (p.u.)
Case 1 - UPF						
ESGA	30; 24; 13	1.0536 / 1; 1.0913 / 1; 0.8017 / 1	72.7869 (65.50%)	0.0151	1.1357	0.8805
SGA	14; 24; 30	0.7708 / 1; 1.0970 / 1; 1.0659 / 1	72.7910 (65.50%)	0.0151	1.1358	0.8805
ABC	30; 24; 13	0.9763 / 1; 1.1559 / 1; 0.8229 / 1	72.9888 (65.41%)	0.0157	1.1449	0.8734
PSO	30; 14; 24	1.0636 / 1; 0.7723 / 1; 1.0932 / 1	72.7914 (65.50%)	0.0151	1.1361	0.8802
GA	24; 14; 30	1.0992 / 1; 0.7705 / 1; 1.0668 / 1	72.7911 (65.50%)	0.0151	1.1356	0.8806
KHA [21]	13; 25; 30	0.8107 / 1; 0.8368 / 1; 0.8410 / 1	75.412 (64.26%)	-	1.1726	0.8528
MGSA-EE [25]	13; 24; 30	0.7978 / 1; 1.0802 / 1; 1.0541 / 1	72.79 (65.50%)	0.0153	-	-
AEO [27]	13; 24; 30	0.7110 / 1; 0.9260 / 1; 1.0900 / 1	73.5988 (65.12%)	-	-	-
CrSA [28]	-	-	74.632 (64.62%)	-	-	-
WSA [28]	-	-	72.789 (65.50%)	-	-	-
ASBO [28]	-	-	72.938 (65.43%)	-	-	-
SFS [33]	13; 24; 30	0.8020 / 1; 1.0920 / 1; 1.0537 / 1	72.785 (65.50%)	0.0151	1.1357	0.8805
QOSIMBO-Q [35]	14; 24; 30	0.7708 / 1; 1.0965 / 1; 1.0655 / 1	72.8 (65.50%)	0.0151	1.1358	0.8804
QOTLBO [36]	12; 24; 29	0.8808 / 1; 1.0592 / 1; 1.0714 / 1	74.101 (64.88%)	0.0160	1.1552	0.8656
Case 2 - OPF						
ESGA	30; 24; 13	1.4433 / 0.7133; 1.1883 / 0.9005; 0.8774 / 0.9050	11.7410 (94.44%)	0.0006	1.0322	0.9688
SGA	14; 25; 30	0.8727 / 0.9030; 0.8988 / 0.9390; 1.4392 / 0.6790	12.9667 (93.85%)	0.0009	1.0391	0.9624
ABC	25; 12; 30	0.9456 / 0.8261; 0.9736 / 0.9437; 1.3719 / 0.7425	14.1392 (93.30%)	0.0016	1.0643	0.9396
PSO	24; 13; 30	1.0927 / 0.7051; 0.8886 / 0.9159; 1.3643 / 0.6890	13.9829 (93.37%)	0.0012	1.0400	0.9615
GA	24; 12; 30	0.9615 / 0.8958; 0.9907 / 0.9049; 1.4370 / 0.7209	12.9208 (93.88%)	0.0009	1.0507	0.9517
CrSA [28]	-	-	17.993 (91.47%)	-	-	-
WSA [28]	-	-	11.961 (94.33%)	-	-	-
ASBO [28]	-	-	14.766 (93.00%)	-	-	-
AM-PSO [31]	13; 24; 30	0.873 / 0.90; 1.186 / 0.89; 1.439 / 0.71	11.7 (94.45%)	-	-	-
EA-OPF [32]	13; 24; 30	0.8824 / 0.90; 1.1888 / 0.90; 1.4510 / 0.71	11.74 (94.44%)	-	-	-
SFS [33]	13; 24; 30	0.8768 / 0.904; 1.1553 / 0.892; 1.4549 / 0.716	11.762 (94.43%)	0.0006	1.0319	0.9691

TABLE 2. Simulation results of different approaches for Scenario II of 33-bus RDN.

Approaches	Bus	S_{DG}(MVA) / pf	P_L (kW)	VD (p.u.)	VSI^{-1} (p.u.)	Min VSI (p.u.)	FF (p.u.)
Case 1 - UPF							
ESGA	24; 13; 30	1.1310 / 1; 0.9564 / 1; 1.2935 / 1	77.0419	0.0065	1.0908	0.9168	0.6490
SGA	13; 25; 30	0.9593 / 1; 1.0271 / 1; 1.2945 / 1	77.9468	0.0067	1.0922	0.9156	0.6545
ABC	24; 30; 13	1.1239 / 1; 1.3262 / 1; 1.0071 / 1	79.0174	0.0051	1.0834	0.9230	0.6505
PSO	6; 31; 14	1.3418 / 1; 0.8407 / 1; 0.7704 / 1	82.2441	0.0061	1.0805	0.9255	0.6693
GA	24; 30; 14	0.8899 / 1; 1.3356 / 1; 0.9063 / 1	77.0828	0.0073	1.0920	0.9158	0.6530
GA/PSO [29]	11; 16; 32	0.9250 / 1; 0.8630 / 1; 1.2000 / 1	103.4	0.0124	1.0517	0.9508	0.7912
GA/IWD [30]	11; 16; 32	1.2214 / 1; 0.6833 / 1; 1.2135 / 1	110.51	0.0069	1.05012	0.9523	0.7999
SFS [33]	13; 24; 30	0.9647 / 1; 1.1337 / 1; 1.3018 / 1	77.410	0.0062	1.0891	0.9182	0.6491
CSOS [34]	14; 24; 30	0.7540 / 1; 1.0990 / 1; 1.0720 / 1	71.4	0.0123	1.1225	0.8909	0.6557
QOSIMBO-Q [35]	7; 13; 31	1.3465 / 1; 1.3043 / 1; 1.5000 / 1	97.1	0.0009	1.0383	0.9631	0.7066
QOTLBO [36]	13; 26; 30	1.0830 / 1; 1.1187 / 1; 1.1990 / 1	103.4	0.0011	1.0493	0.9530	0.7400
Case 2 - OPF							
ESGA	30; 13; 24	1.4700 / 0.7145; 0.9229 / 0.9028; 1.1922 / 0.9015	11.9008	0.00034	1.0243	0.9763	0.2971
SGA	30; 13; 24	1.5821 / 0.7354; 0.9045 / 0.8970; 0.7683 / 0.6794	15.6631	0.00053	1.0349	0.9663	0.3183
ABC	24; 14; 29	1.4309 / 0.9693; 0.9031 / 0.8739; 1.5806 / 0.7958	17.6691	0.00039	1.0234	0.9771	0.3244
PSO	24; 14; 30	1.2360 / 0.6647; 0.8365 / 0.8955; 1.5568 / 0.7346	14.8569	0.00042	1.0297	0.9712	0.3127
GA	14; 24; 30	0.7462 / 0.9105; 0.9814 / 0.8988; 1.6985 / 0.7336	13.8012	0.00092	1.0362	0.9651	0.3115
SFS [33]	13; 24; 30	0.9214 / 0.905; 1.1900 / 0.895; 1.4746 / 0.718	11.911	0.00033	1.0243	0.9763	0.2971

cases of power factors, the optimal results from ESGA are compared to those from other approaches in previous studies, which are presented in Table 1. Case 1 shows that ESGA reduces the active power loss to 72.7869 kW after installing DG units, which corresponds to a power loss reduction of 65.50%. The power loss reduction achieved by ESGA in Case 1 is lower compared to the ABC, KHA [21], AEO [27], CrSA [28], ASBO [28], QOSIMBO-Q [35], and QOTLBO [36] methods, and is close to the result of the SGA, PSO, GA, MGSA-EE [25], WSA [28], and SFS [33]. In Case 2, ESGA achieves a minimum active power loss of 11.7410 kW,

resulting in a power loss reduction of 94.44%. This result is lower than those from SGA, ABC, PSO, GA, CrSA [28], WSA [28], ASBO [28], and SFS [33], and is similar to those from AM-PSO [31], and EA-OPF [32] methods.

Compared with Case 1, a higher active power loss reduction in Case 2 is apparent in Table 1, which corresponds to the scenario where DG units are functioning at their optimal power factors. This suggests that installing optimal DG power factors can greatly reduce power loss in the system. Moreover, Fig. 3 reveals that ESGA has superior convergence speeds for all cases compared to SGA, ABC, PSO, and GA.
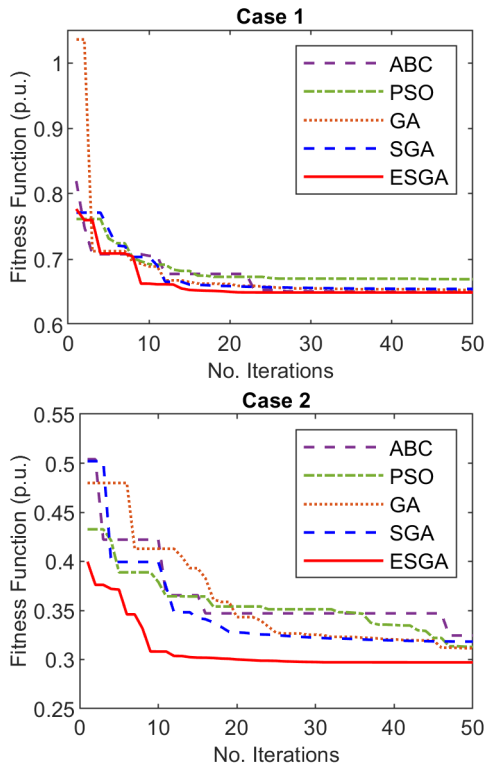
FIGURE 4. Convergence characteristics of ESGA and other methods for Scenario II of 33-bus RDN.
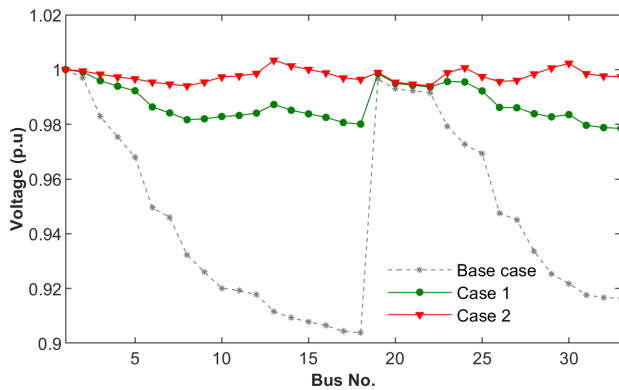

FIGURE 5. Voltage profile of the 33-bus RDN in Scenario II.

FIGURE 6. VSI values of the 33-bus RDN in Scenario II.
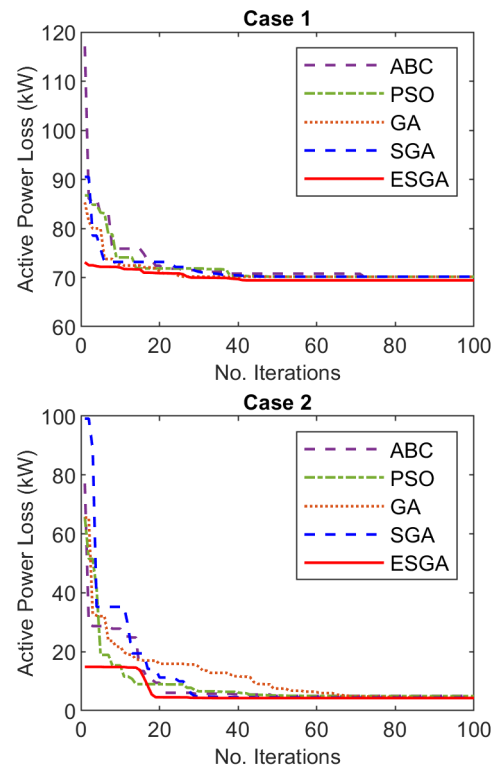
FIGURE 7. Convergence characteristics of ESGA and other methods for Scenario I of 69-bus RDN.

2) SCENARIO II

In this scenario, the ODGP problem simultaneously optimizes active power loss, *VD*, and VSI. Table 2 displays the findings for two operating conditions of DG units using ESGA, SGA, and other techniques. In Case 1, ESGA achieves an active power loss of 77.0419 kW, a *VD* value of 0.0065 p.u., and a VSI^{-1} value of 1.0908 p.u. Based on the results in Case 1, ESGA obtains a superior fitness function value in comparison to SGA, ABC, PSO, GA, GA/PSO [29], GA/IWD [30], CSOS [34], QOSIMBO-Q [35], and QOTLBO [36]. The result achieved by ESGA is nearly identical to that achieved by SFS [33]. In Case 2, ESGA
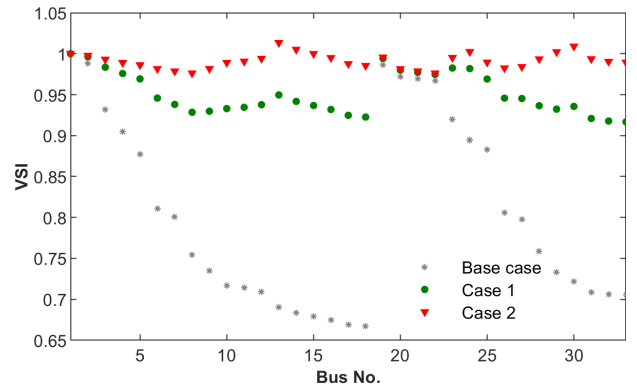
produces an active power loss of 11.9008 kW, a *VD* value of 0.00034 p.u., and a VSI^{-1} value of 1.0243 p.u., which are similar to that achieved by SFS [33]. ESGA obtains better results than other methods for Case 2.

From Table 2, Case 2 delivers better results for all three objective functions than Case 1. This suggests that incorporating optimal DG power factors significantly enhances active power loss, *VD*, and VSI^{-1}. Fig. 4 demonstrates the convergence patterns of ESGA and other methods in Scenario II. For all cases, ESGA outperforms SGA, ABC, PSO, and GA in terms of convergence ability. Figs. 5 and 6 display the voltage profiles and VSI values of 33-bus RDN for Cases
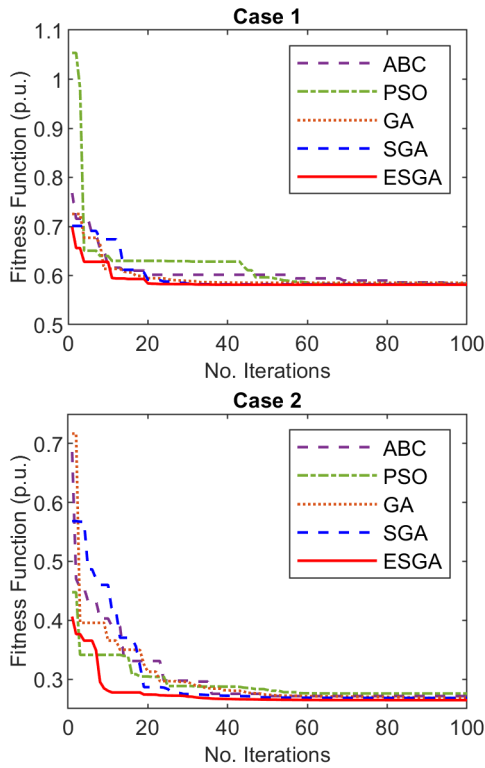
FIGURE 8. Convergence characteristics of ESGA and other methods for Scenario II of 69-bus RDN.
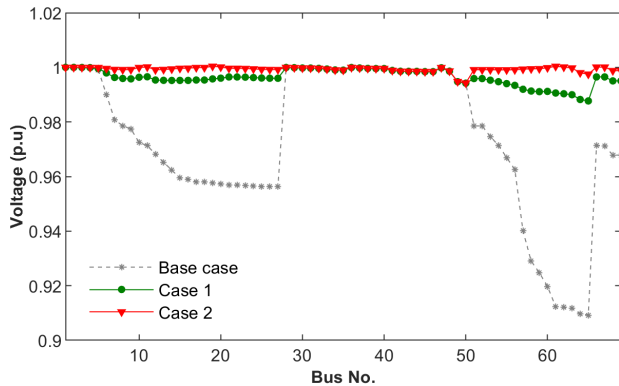

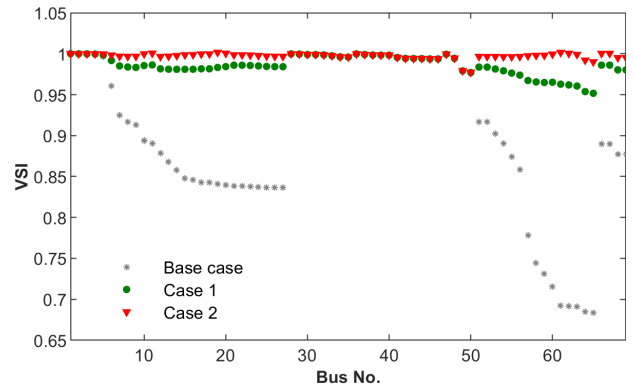FIGURE 9. Voltage profile of the 69-bus RDN in Scenario II.

FIGURE 10. VSI values of the 69-bus RDN in Scenario II.
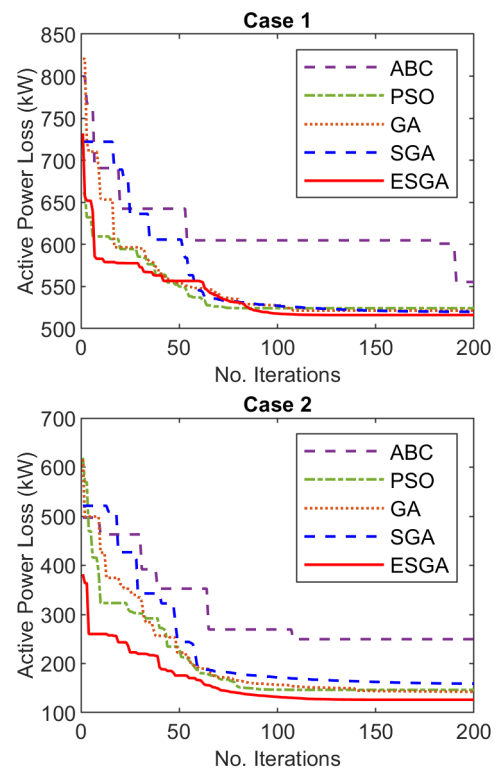
FIGURE 11. Convergence characteristics of ESGA and other methods for Scenario I of 118-bus RDN.

1 and 2, respectively. It can be shown that Case 2 leads to a notable improvement in voltage profile and VSI.

B. 69-BUS RDN
A medium-scale 69-bus RDN [44] is used to test the ESGA in this section. The maximum iteration (G^{max}) of ESGA is set to 100. Before DGs integration, the system has an active power loss of 224.9917 kW, a *VD* value of 0.0993 p.u., and a VSI^{-1} value of 1.4635 p.u. Three DG units are installed in this system.

1) SCENARIO I
Table 3 displays the results attained by ESGA, SGA, and other techniques for two cases in Scenario I, where only

active power loss is considered. For Case 1, ESGA identifies an active power loss of 69.4260 kW (69.14% reduction), which is nearly identical to MGSA-EE [25], WSA [28], ASBO [28], and SFS [26] and lower than other methods. For Case 2, the active power loss attained by ESGA is 4.2676 kW (98.10% reduction), which is lower than the values produced by SGA, ABC, PSO, GA, CrSA [28], WSA [28], ASBO [28], and SFS [33]. It is evident that the active power loss in Case 2 is significantly lower than that in Case 1. This suggests that optimal DG power factors lead to a remarkable improvement in the active power loss of the system. Moreover, the convergence curves of ESGA, SGA,

TABLE 3. Simulation results of different approaches for Scenario I of 69-bus RDN.

Approaches	Bus	S_{DG}(MVA) / pf	P_L (kW)/ (PLR)	VD (p.u.)	VSI^{-1} (p.u.)	Min VSI (p.u.)
Case 1 - UPF						
ESGA	18; 11; 61	0.3804 / 1; 0.5268 / 1; 1.7190 / 1	69.4260 (69.14%)	0.0052	1.0887	0.9185
SGA	17; 61; 53	0.4665 / 1; 1.6845 / 1; 0.5466 / 1	70.1752 (68.81%)	0.0054	1.0886	0.9186
ABC	8; 61; 17	0.5758 / 1; 1.7433 / 1; 0.4107 / 1	70.1589 (68.82%)	0.0057	1.0837	0.9227
PSO	61; 17; 50	1.7812 / 1; 0.5312 / 1; 0.7202 / 1	70.1579 (68.82%)	0.0061	1.0889	0.9183
GA	50; 17; 61	0.7202 / 1; 0.5311 / 1; 1.7812 / 1	70.1579 (68.82%)	0.0061	1.0889	0.9183
KHA [21]	12; 22; 61	0.4962 / 1; 0.3113 / 1; 1.7354 / 1	69.563 (69.08%)	-	1.0887	0.9185
MGSA-EE [25]	11; 18; 61	0.5446 / 1; 0.3792 / 1; 1.7240 / 1	69.40 (69.15%)	0.0050	-	-
CrSA [28]	-	-	71.262 (68.33%)	-	-	-
WSA [28]	-	-	69.4287 (69.14%)	-	-	-
ASBO [28]	-	-	69.433 (69.14%)	-	-	-
SFS [33]	11; 18; 61	0.5273 / 1; 0.3805 / 1; 1.7198 / 1	69.428 (69.14%)	0.0052	1.0886	0.9186
QOSIMBO-Q [35]	9; 18; 61	0.8336 / 1; 0.4511 / 1; 1.5000 / 1	71 .0 (68.44%)	0.0071	1.1131	0.8984
QOTLBO [36]	18; 61; 63	0.5334 / 1; 1.1986 / 1; 0.5672 / 1	71.625 (68.17%)	0.0062	1.0874	0.9196
Case 2 - OPF						
ESGA	18; 61; 11	0.4549 / 0.8333; 2.0573 / 0.8139; 0.6081 / 0.8132	4.2676 (98.10%)	0.00013	1.0233	0.9773
SGA	61; 19; 11	2.0581 / 0.8176; 0.4449 / 0.8700; 0.6214 / 0.7064	4.3677 (98.06%)	0.00012	1.0233	0.9773
ABC	61; 18; 66	2.0328 / 0.8112; 0.4181 / 0.7737; 0.4870 / 0.8558	4.9807 (97.79%)	0.00058	1.0233	0.9772
PSO	17; 50; 61	0.6304 / 0.8282; 0.8844 / 0.8138; 2.1310 / 0.8139	4.9209 (97.81%)	0.00038	1.0230	0.9775
GA	11; 61; 17	0.6338 / 0.8497; 2.0604 / 0.8082; 0.4318 / 0.8070	4.3098 (98.08%)	0.00016	1.0233	0.9773
CrSA [28]	-	-	8.824 (96.08%)	-	-	-
WSA [28]	-	-	4.844 (97.85%)	-	-	-
ASBO [28]	-	-	4.727 (97.90%)	-	-	-
SFS [33]	11; 21; 61	0.6921 / 0.819; 0.4031 / 0.833; 2.0484 / 0.818	4.298 (98.09%)	0.00012	1.0233	0.9773

TABLE 4. Simulation results of different approaches for Scenario II of 69-bus RDN.

Approaches	Bus	S_{DG}(MVA) / pf	P_L (kW)	VD (p.u.)	VSI^{-1} (p.u.)	Min VSI (p.u.)	FF (p.u.)
Case 1 - UPF							
ESGA	11; 61; 21	0.6426 / 1; 1.9474 / 1; 0.4196 / 1	72.1273	0.0016	1.0508	0.9517	0.5812
SGA	18; 10; 61	0.4797 / 1; 0.6098 / 1; 1.9430 / 1	72.2504	0.0016	1.0507	0.9517	0.5819
ABC	19; 12; 61	0.4261 / 1; 0.5905 / 1; 2.0086 / 1	73.7873	0.0010	1.0431	0.9587	0.5837
PSO	66; 61; 18	0.5278 / 1; 1.9567 / 1; 0.4851 / 1	72.4164	0.0016	1.0506	0.9518	0.5828
GA	61; 18; 53	1.9017 / 1; 0.5634 / 1; 0.6504 / 1	72.9241	0.0016	1.0506	0.9518	0.5852
GA/PSO [29]	21; 61; 63	0.9100 / 1; 1.1930 / 1; 0.8850 / 1	81.1	0.0031	1.0238	0.9768	0.6240
GA/IWD [30]	20; 61; 64	0.9115 / 1; 1.3926 / 1; 0.8059 / 1	80.91	0.0029	1.0190	0.9814	0.6208
SFS [33]	11; 19; 61	0.5703 / 1; 0.4661 / 1; 1.9674 / 1	72.445	0.0014	1.0485	0.9537	0.5814
CSOS [34]	17; 61; 64	0.5370 / 1; 1.2000 / 1; 0.5360 / 1	71.5	0.0063	1.0842	0.9223	0.6151
QOSIMBO-Q [35]	61; 15; 63	1.4385 / 1; 0.7754 / 1; 0.7235 / 1	79.7	0.0007	1.0237	0.9768	0.6033
QOTLBO [36]	15; 61; 63	0.8110 / 1; 1.1470 / 1; 1.0020 / 1	80.5	0.0007	1.0236	0.9769	0.6068
Case 2 - OPF							
ESGA	61; 11; 19	2.0658 / 0.8147; 0.6343 / 0.8038; 0.4455 / 0.8385	4.2899	0.00010	1.0233	0.9773	0.2644
SGA	50; 18; 61	0.7693 / 0.7230; 0.6808 / 0.8317; 2.1597 / 0.8150	5.1455	0.00024	1.0186	0.9817	0.2680
ABC	11; 18; 61	0.3802 / 0.6635; 0.5945 / 0.7814; 2.1122 / 0.8536	5.7660	0.00015	1.0233	0.9773	0.2712
PSO	13; 61; 49	0.9804 / 0.8496; 2.1072 / 0.8129; 0.9747 / 0.8121	6.9778	0.00021	1.0175	0.9828	0.2756
GA	50; 61; 15	0.8235 / 0.7550; 2.1340 / 0.8173; 0.7301 / 0.8330	5.3968	0.00020	1.0158	0.9845	0.2681
SFS [33]	11; 18; 61	0.6111 / 0.811; 0.4708 / 0.835; 2.0664 / 0.816	4.285	0.00010	1.0233	0.9773	0.2644

ABC, PSO, and GA in Fig. 7 illustrate that ESGA has a faster convergence speed than other methods.

2) SCENARIO II

ESGA is utilized to solve the ODGP problem with three objectives, namely active power loss, VD, and maximizing VSI in this scenario. The results found by ESGA, SGA, and other methods are presented in Table 4 for two different power factor values of DG units. For Case 1, ESGA achieves an active power loss value of 72.1273 kW, a VD value of 0.0016 p.u., and a VSI^{-1} value of 1.0508 p.u., which leads to a fitness function value of 0.5812. As shown in Table 4, ESGA exhibits better performance in terms of fitness function value than SGA, ABC, PSO, GA, GA/PSO [29], GA/IWD [30], SFS [33], CSOS [34], QOSIMBO-Q [35], and QOTLBO [36]. In Case 2, the fitness function value from ESGA is slightly better than that of SGA, ABC, PSO, and GA, and

similar to SFS [33]. Therefore, ESGA offers a competitive compromise solution for the multi-objective ODGP problem of the 69-bus RDN. The convergence characteristics of ESGA, SGA, ABC, PSO, and GA are shown in Fig. 8. It is evident that ESGA outperforms SGA, ABC, PSO, and GA in terms of convergence ability for both cases. The results demonstrate that optimal DGs power factors (Case 2) lead to a substantial enhancement in all three objectives in comparison with Case 1. Moreover, as shown in Fig. 9 and Fig. 10, the voltage profile and VSI values in Case 2 are better than that in Case 1.

C. 118-BUS RDN

The effectiveness of the suggested ESGA with a large-scale system is verified by testing it on the 118-bus RDN [45]. Its maximum iteration (G^{max}) is set to 200. Without any DGs installed, 118-bus RDN has an active power loss of

TABLE 5. Simulation results of different approaches for Scenario I of 118-bus RDN.

Approaches	Bus	S_{DG}(MVA) / pf	P_L (kW) / (PLR)	VD (p.u.)	VSI^{-1} (p.u.)	Min VSI (p.u.)
Case 1 - UPF						
ESGA	42; 30; 80; 96; 50; 72; 109	1.1543 / 1; 3.7082 / 1; 2.0949 / 1; 1.6631 / 1; 2.3337 / 1; 2.5333 / 1; 3.1199 / 1	516.1280 (60.24%)	0.0588	1.2043	0.8304
SGA	50; 31; 80; 42; 110; 73; 96	1.9711 / 1; 2.9972 / 1; 1.9497 / 1; 1.2288 / 1; 2.8508 / 1; 2.4148 / 1; 1.6473 / 1	520.0249 (59.94%)	0.0608	1.2103	0.8262
ABC	19; 110; 87; 90; 74; 48; 41	1.9941 / 1; 3.2312 / 1; 1.2487 / 1; 2.7061 / 1; 2.4620 / 1; 2.6719 / 1; 1.3591 / 1	555.3944 (57.21%)	0.0592	1.2494	0.8004
PSO	50; 80; 96; 109; 72; 58; 41	2.7167 / 1; 2.0949 / 1; 1.6631 / 1; 3.1199 / 1; 2.5333 / 1; 0.9134 / 1; 1.8050 / 1	524.2670 (59.61%)	0.0597	1.2058	0.8293
GA	29; 20; 110; 96; 50; 80; 72	5 / 1; 1.6659 / 1; 2.8685 / 1; 1.6598 / 1; 2.5504 / 1; 2.0928 / 1; 2.5513 / 1	521.3599 (59.84%)	0.0604	1.2047	0.8301
KHA [21]	48; 53; 74; 80; 96; 109; 112	1.7242 / 1; 1.3356 / 1; 1.8623 / 1; 1.8653 / 1; 1.6631 / 1; 1.9473 / 1; 1.1848 / 1	574.7097 (55.73%)	-	1.2433	0.8043
SFS [33]	21; 42; 50; 71; 81; 97; 110	1.3757 / 1; 1.1997 / 1; 2.7418 / 1; 2.8915 / 1; 1.7025 / 1; 1.3321 / 1; 2.6674 / 1	525.277 (59.53%)	0.06118	1.2090	0.8271
QOTLBO [36]	24; 42; 47; 74; 78; 94; 108	1.2463 / 1; 0.7322 / 1; 3.5392 / 1; 2.6792 / 1 ; 1.2483 / 1; 1.0865 / 1; 3.2432 / 1	576.1823 (55.61%)	0.0629	1.2093	0.8269
Case 2 - OPF						
ESGA	80; 50; 110; 41; 20; 96; 74	2.6166 / 0.7968; 3.6676 / 0.7389; 3.6350 / 0.7703; 2.2171 / 0.8206; 2.1892 / 0.8162; 1.9846 / 0.8413; 2.7335 / 0.8406	126.2267 (90.28%)	0.0074	1.1020	0.9074
SGA	110; 50; 80; 96; 41; 72; 20	3.5915 / 0.7659; 3.2921 / 0.7398; 2.9508 / 0.7996; 1.4533 / 0.3066; 2.3228 / 0.6582; 3.0505 / 0.8561; 1.8949 / 0.5940	159.0576 (87.75%)	0.0119	1.1044	0.9055
ABC	108; 80; 96; 73; 52; 20; 45	3.8202 / 0.6751; 2.7630 / 0.8064; 2.3927 / 0.5726; 3.0015 / 0.9773; 3.8148 / 0.6958; 3.3661 / 0.7329; 1.5148 / 1	249.6251 (80.77%)	0.0086	1.1057	0.9044
PSO	110; 58; 74; 30; 80; 50; 96	3.6349 / 0.7703; 1.0692 / 0.7657; 2.7335 / 0.8406; 4.7193 / 0.8029; 2.6163 / 0.7968; 3.1468 / 0.7297; 1.9847 / 0.8413	146.3163 (88.73%)	0.0153	1.1448	0.8735
GA	96; 72; 50; 42; 110; 81; 32	1.9235 / 0.8311; 2.9606 / 0.8451; 2.6315 / 0.6852; 1.2477 / 0.8446; 3.6612 / 0.7738; 2.2306 / 0.8011; 2.8586 / 0.8234	142.2735 (89.04%)	0.0136	1.1364	0.8800
SFS [33]	20; 41; 50; 74; 80; 96; 110	2.1896 / 0.816; 2.2188 / 0.820; 3.6692 / 0.739; 2.7330 / 0.841; 2.6156 / 0.797; 1.9850 / 0.841; 3.6341 / 0.770	126.227 (90.28%)	0.0074	1.1020	0.9075

TABLE 6. Simulation results of different approaches for Scenario II of 118-bus RDN.

Approaches	Bus	S_{DG}(MVA) / pf	P_L (kW)	VD (p.u.)	VSI^{-1} (p.u.)	Min VSI (p.u.)	FF (p.u.)
Case 1 - UPF							
ESGA	96; 50; 109; 20; 73; 42; 80	1.9728 / 1; 3.8929 / 1; 3.4999 / 1; 2.1369 / 1; 2.8380 / 1; 1.4575 / 1; 2.4602 / 1	548.9334	0.0309	1.1277	0.8867	0.6997
SGA	110; 73; 20; 96; 42; 50; 81	3.1580 / 1; 2.8157 / 1; 2.5870 / 1; 2.3136 / 1; 1.4114 / 1; 3.6420 / 1; 1.8003 / 1	548.9967	0.0333	1.1436	0.8744	0.7069
ABC	19; 99; 29; 73; 85; 109; 49	2.6827 / 1; 1.7514 / 1; 2.9098 / 1; 3.1127 / 1; 1.0314 / 1; 3.5640 / 1; 3.2894 / 1	580.4416	0.0455	1.1812	0.8466	0.7590
PSO	31; 73; 80; 50; 110; 96; 42	3.1528 / 1; 2.8380 / 1; 2.4599 / 1; 2.9880 / 1; 3.2131 / 1; 1.9726 / 1; 1.3804 / 1	546.7996	0.0350	1.1355	0.8807	0.7063
GA	73; 110; 42; 51; 80; 91; 31	2.8299 / 1; 3.1205 / 1; 1.3911 / 1; 2.5304 / 1; 2.4235 / 1; 2.1009 / 1; 3.5393 / 1	545.9834	0.0368	1.1356	0.8806	0.7087
SFS [33]	19; 41; 49; 73; 79; 96; 108	2.0313 / 1; 1.9135 / 1; 4.0113 / 1; 2.7996 / 1; 3.0734 / 1; 2.0861 / 1; 3.8194 / 1	564.104	0.0309	1.142	0.8757	0.7140
CSOS [27]	20; 39; 47; 72; 85; 91; 110	1.790 / 1; 2.739 / 1; 1.833 / 1; 2.533 / 1; 1.665 / 1; 2.091 / 1; 2.868 / 1	516.0	0.0466	1.2025	0.8316	0.7155
QOTLBO [36]	43; 49; 54; 74; 80; 94; 111	1.5880 / 1; 3.8459 / 1; 0.9852 / 1; 3.1904 / 1; 3.1632 / 1; 1.9527 / 1; 3.6013 / 1	677.5881	0.0233	1.1372	0.8794	0.7878
Case 2 - OPF							
ESGA	96; 80; 50; 73; 20; 110; 41	2.0124 / 0.8402; 2.6898 / 0.7931; 3.8476 / 0.7371; 2.8785 / 0.8415; 2.3573 / 0.8149; 3.7284 / 0.7733; 2.4487 / 0.8196	128.2423	0.0057	1.0996	0.9094	0.3276
SGA	41; 110; 73; 20; 50; 81; 96	2.1252 / 0.8457; 3.6554 / 0.7704; 2.8685 / 0.8535; 2.1543 / 0.8046; 3.5554 / 0.6650; 1.9893 / 0.6719; 2.3225 / 0.5413	149.4749	0.0082	1.1034	0.9063	0.3489
ABC	71; 41; 108; 72; 11; 90; 49	1.4237 / 0.5432; 1.4015 / 0.7319; 4.1884 / 0.6512; 1.2716 / 0.9959; 2.9962 / 0.5223; 2.9707 / 0.8198; 4.8448 / 0.6222	271.5024	0.0275	1.1476	0.8714	0.4842
PSO	110; 30; 80; 96; 41; 74; 50	3.7285 / 0.7733; 4.6552 / 0.8017; 2.7007 / 0.7932; 2.0328 / 0.8404; 2.0839 / 0.8261; 2.7924 / 0.8408; 3.1508 / 0.7296	131.1355	0.0106	1.1317	0.8836	0.3445
GA	111; 11; 72; 80; 42; 91; 50	3.5632 / 0.7735; 3.6008 / 0.8206; 3.0113 / 0.8395; 2.6541 / 0.7968; 1.5775 / 0.8371; 2.0883 / 0.8340; 3.8814 / 0.7372	148.6137	0.0080	1.1023	0.9072	0.3478
SFS [33]	20; 41; 50; 74; 80; 96; 110	1.4025 / 0.798; 1.4255 / 0.818; 2.6147 / 0.736; 1.5045 / 0.844; 1.6172 / 0.796; 1.1245 / 0.829; 2.3758 / 0.771	128.105	0.0058	1.0995	0.9095	0.3277

1298.0916 kW, a *VD* value of 0.3577 p.u., and a VSI^{-1} value of 1.7552 p.u. The test assumes the installation of seven DG units.

1) SCENARIO I

The results of ESGA, SGA, ABC, PSO, GA, KHA [21], SFS [33], and QOTLBO [36] for Scenario I of 118-bus
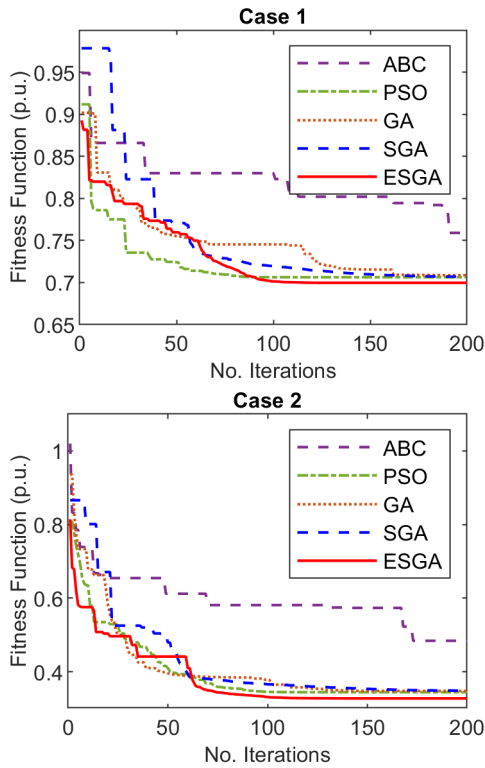
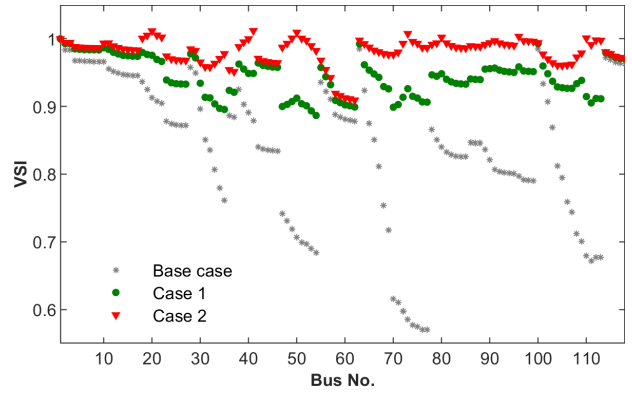**FIGURE 12.** Convergence characteristics of ESGA and other methods for Scenario II of 118-bus RDN.

FIGURE 13. Voltage profile of the 118-bus RDN in Scenario II.
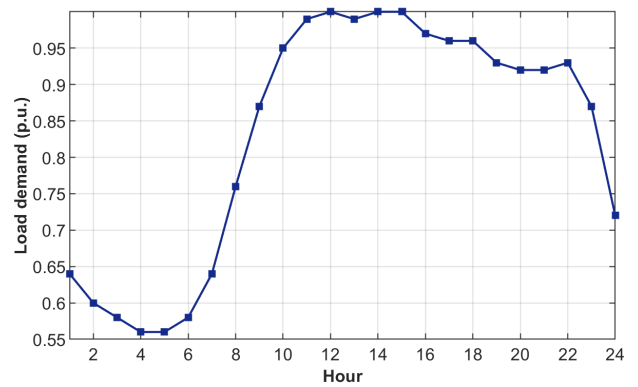

FIGURE 14. VSI values of the 118-bus RDN in Scenario II.

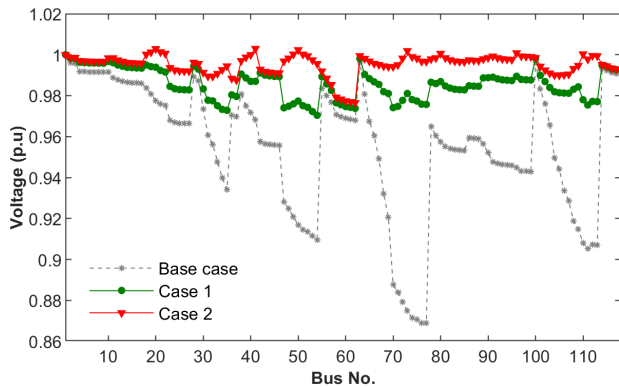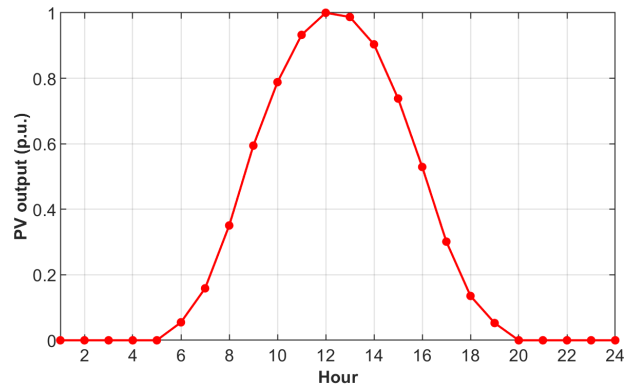**FIGURE 15.** Hourly load demand curve for a representative day.

FIGURE 16. Hourly expected output of a PV DG for a representative day.

RDN are presented in Table 5. For Case 1, ESGA finds an active power loss of 516.1280 kW (a reduction of 60.24%), while for Case 2, the active power loss yielded by ESGA is 126.2267 kW (a reduction of 90.28%). In both cases, the active power loss values yielded by ESGA are superior to those yielded by other compared methods. These results demonstrate the effectiveness of ESGA in resolving the ODGP with a large-scale system in Scenario I. According to Table 5, ESGA obtains a significantly better active power loss value in Case 2 compared to Case 1, indicating that installing optimal DGs power factors can suggestively reduce the active power loss of RDN. Furthermore, Fig. 11 illustrates

the convergence curves of ESGA and other methods, showing a faster convergence speed of ESGA.

2) SCENARIO II

To address the ODGP problem in this scenario, ESGA is utilized for the concurrent minimization of active power loss, VD, and VSI^{-1}. Table 6 gives the results of simulations yielded by ESGA, SGA, and other methods. The ESGA produces an active power loss of 548.9334 kW, a VD value of 0.0309 p.u., and a VSI^{-1} of 1.1277 p.u. for Case 1. For Case 2,
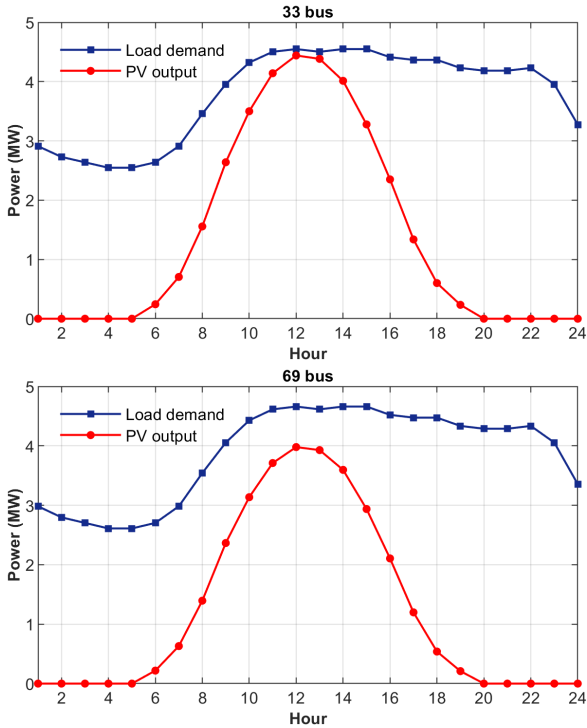
FIGURE 17. Hourly power output of PV DGs corresponds to hourly load demand of 33-bus and 69-bus RDNs.

FIGURE 18. Hourly power loss of 33-bus and 69-bus RDNs with and without DG integration.

TABLE 7. Mean and standard deviation of solar irradiance.

Hour	$\mu(kW/m^2)$	$\sigma(kW/m^2)$	Hour	$\mu(kW/m^2)$	$\sigma(kW/m^2)$
6	0.019	0.035	13	0.648	0.282
7	0.096	0.11	14	0.59	0.265
8	0.222	0.182	15	0.477	0.237
9	0.381	0.217	16	0.338	0.204
10	0.511	0.253	17	0.19	0.163
11	0.61	0.273	18	0.08	0.098
12	0.657	0.284	19	0.017	0.032

the corresponding values are 128.2423 kW, 0.0057 p.u., and 1.0996 p.u. From Table 6, active power loss, VD, and VSI^{-1} values in Case 2 are better than those in Case 1. This signifies that the installations of optimal DG power factors provide a significant enhancement in all three considered objectives.

The results of the simulation for the multi-objective scenario of 118-bus RDN are presented in Table 6. In Case 1, ESGA outperforms SGA, ABC, PSO, GA, SFS [33], CSOS [34], and QOTLBO [36] in terms of the fitness function value. In Case 2, ESGA achieves a lower fitness function value than SGA, ABC, PSO, and GA. The fitness function value obtained by ESGA is the minimum value among all compared methods for each case. Therefore, the ESGA method offers a competitive solution to the multi-objective ODGP problem of 118-bus RDN.

In Fig. 12, the convergence curves of ESGA, SGA, ABC, PSO, and GA are presented, and it is inferred that ESGA has a faster convergence speed than other compared methods. In addition, Figs. 13 and 14 display the voltage profile and VSI values of the 118-bus RDN, respectively, which shows that Case 2 leads to a considerable enhancement in the voltage profile and VSI of the RDN.

D. CONSIDERATION OF DAILY VARIABLE LOAD AND PV DG UNCERTAINTY FOR THE ODGP PROBLEM

In this section, the ODGP problem is investigated in a scenario that considers daily variable load and DG uncertainty. Assume that three PV DGs are integrated into the RDN. This investigation is performed on the 33-bus and 69-bus RDNs.
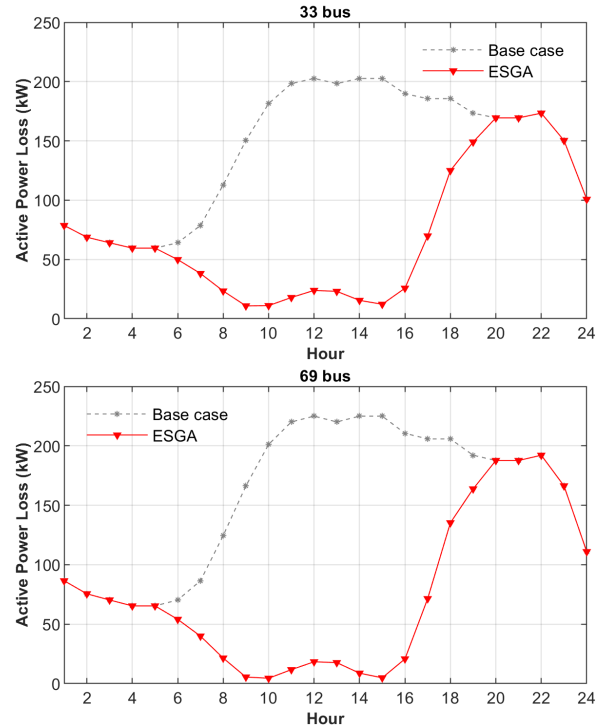
In this scenario, the objective function of the ODGP problem is to minimize daily energy loss for a representative day with 24 hours ($T = 24$) and a time step (Δt) of 1 hour [46]:

$$E_{loss} = \sum_{t=1}^{24} P_L(t) \times \Delta t \qquad (31)$$

where $P_L(t)$ is the active power loss at time t.

The hourly load demand curve for a representative day is depicted in Fig. 15, which is taken from [47]. At each time t, power load demands of the RDN vary with the load factor (in Fig. 15) as follows [47]:

$$P_D(t) = P_{D,base} \times \lambda(t) \qquad (32)$$

$$Q_D(t) = Q_{D,base} \times \lambda(t) \qquad (33)$$

where $P_{D,base}$ and $Q_{D,base}$ denote the initial active and reactive power demands, respectively.

Since solar irradiance primarily governs the output power of PV DGs, the Beta probability density function (PDF) can be applied to simulate the stochastic behavior of solar

TABLE 8. Simulation results of 33-bus and 69-bus RDNs considering daily variable load and PV DG uncertainty.

Approaches	Bus	S_{DG}(MVA) / pf	E_{loss} (kW)	PLR
33-bus				
ESGA	24; 14; 30	1.5096/ 0.9007; 1.0581/ 0.9056; 1.8732/ 0.7165	1689.1032	50.62%
SGA	13; 24; 30	1.1138/ 0.8567; 1.2071/ 0.6542; 1.8190/ 0.7380	1720.3623	49.70%
69-bus				
ESGA	61; 11; 21	2.6405/ 0.8147; 0.8110/ 0.8161; 0.5276/ 0.8321	1785.8079	52.83%
SGA	61; 19; 53	2.6201/ 0.8251; 0.7013/ 0.8523; 0.6822/ 0.5433	1800.2544	52.45%

FIGURE 19. Voltage profile of 33-bus and 69-bus RDNs without DG integration for a representative day.
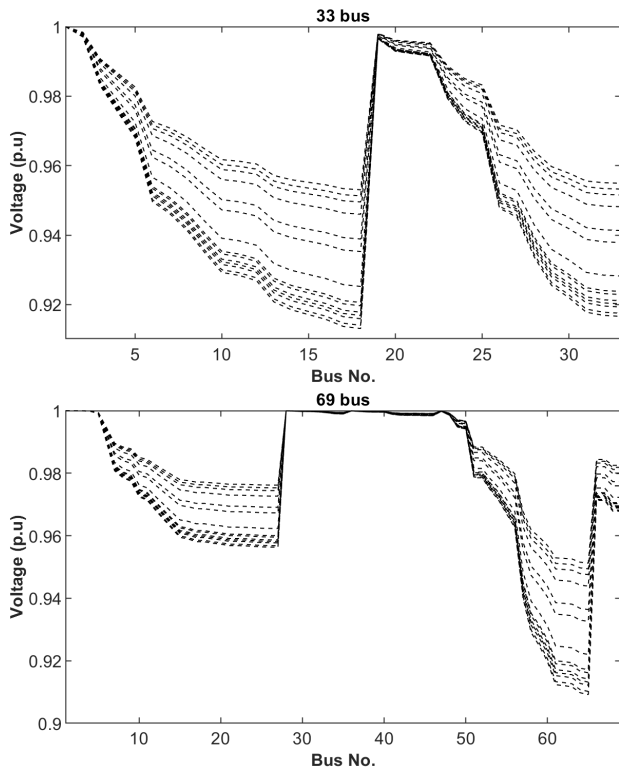

FIGURE 20. Voltage profile of 33-bus and 69-bus RDNs with DG integration for a representative day.

irradiation as follows [47], [48]:

$$f_s(s) = \begin{cases} \dfrac{\Gamma(\alpha + \beta)}{\Gamma(\alpha)\Gamma(\beta)} s^{(\alpha-1)}(1-s)^{(\beta-1)} & 0 \le s \le 1; \alpha, \beta \ge 0 \\ 0 & \text{otherwise} \end{cases}$$

(34)

where s represents the random variable of solar irradiance (kW/m^2), α and β represent parameters of beta PDF which can be defined based on mean (μ) and standard deviation (σ) of historical solar irradiance data in the following equation [47], [48]:

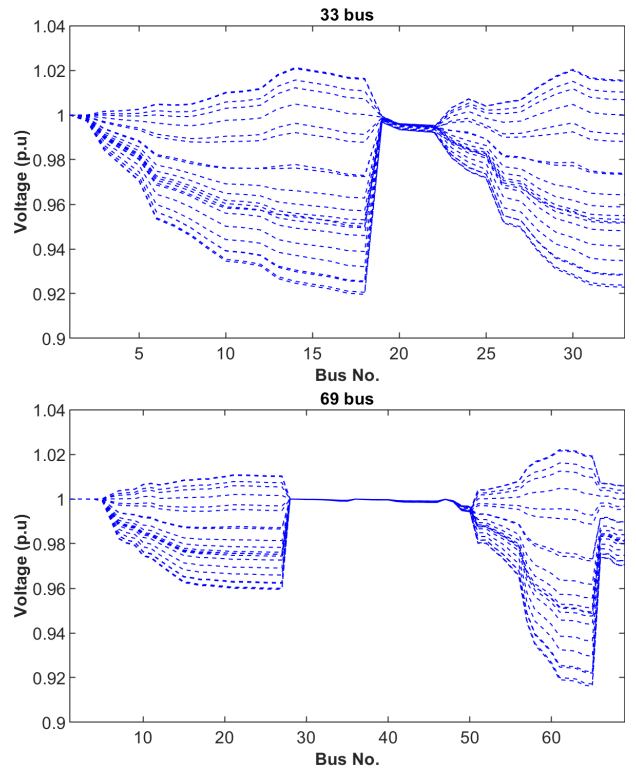$$\beta = (1 - \mu)\left(\frac{\mu(1+\mu)}{\sigma^2} - 1\right)$$

(35)

$$\alpha = \frac{\mu \times \beta}{1 - \mu}$$

(36)

The expected output for a given time t is determined as follows [47], [48]:

$$P_{PV}(t) = \int_0^1 P_o(s) f_b(s)\, ds$$

(37)

where

$$P_o(s) = N_{PV} \times FF \times V_y \times I_y$$

(38)

$$FF = \frac{V_{MPP} \times I_{MPP}}{V_{oc} \times I_{sc}}$$

(39)

$$V_y = V_{oc} - K_v \times T_{cy}$$

(40)

$$I_y = s[I_{sc} + K_i \times (T_c - 25)]$$

(41)

$$T_{cy} = T_A + s\left(\frac{N_{OT} - 20}{0.8}\right)$$

(42)

where N_{PV} denotes the number of PV modules, I_{MPP} and V_{MPP} are the current and voltage at the maximum power point, respectively, I_{SC} denotes short-circuit current, V_{oc} denotes the open-circuit voltage, K_i and K_v denote the current and voltage temperature coefficients, respectively, T_A denotes the ambient temperature, and N_{OT} denotes the nominal operating temperature of the cell.

The mean and standard deviation for each hour of the 24-hour day are shown in Table 7, which are computed based on the historical data taken from [47], [48]. The specifications of the PV module used in the PV model can be given as

TABLE 9. Simulation results of different approaches for 23 benchmark functions.

Function	ESGA		GSA [49]		PSO [49]		GWO [49]		WOA [50]	
	Mean	Std	Mean	Std	Mean	Std	Mean	Std	Mean	Std
F1	6.95E-11	2.52E-16	2.53E-11	9.67E-17	1.36E-04	2.02E-04	6.59E-28	6.34E-05	1.41E-30	4.91E-30
F2	0.0319	0.1114	0.0557	0.1941	0.0421	0.0454	7.18E-17	0.0290	1.06E-21	2.39E-21
F3	2.08E-04	1.34E-04	896.5347	318.9559	70.1256	22.1192	3.29E-06	79.1496	5.39E-07	2.93E-06
F4	0.1425	0.0515	7.3549	1.7415	1.0865	0.3170	5.61E-07	1.3151	0.0726	0.3975
F5	26.8032	1.7872	67.5431	62.2253	96.7183	60.1156	26.8126	69.9050	27.8656	0.7636
F6	1.01E-10	3.81E-11	2.5E-16	1.74E-16	1.02E-04	8.28E-05	0.8166	1.26E-04	3.1163	0.5324
F7	0.5405	0.2865	0.0894	0.0434	0.1229	0.0450	0.0022	0.1003	0.0014	0.0011
F8	-8921.95	669.65	-2821.07	493.04	-4841.29	1152.81	-6123.10	-4087.44	-5080.76	695.80
F9	38.2065	7.4895	25.9684	7.4701	46.7042	11.6294	0.3105	47.3561	0	0
F10	0.0506	0.0112	0.0621	0.2363	0.2760	0.5090	1.06E-13	0.0778	7.4043	9.8976
F11	0.0037	0.0059	27.7015	5.0403	0.0092	0.0077	0.0045	0.0067	0.0003	0.0016
F12	1.46E-04	5.04E-05	1.7996	0.9511	0.0069	0.0263	0.0534	0.0207	0.3397	0.2149
F13	0.0011	0.0034	8.8991	7.1262	0.0067	0.0089	0.6545	0.0045	1.8890	0.2661
F14	0.9980	5.83E-17	5.8598	3.8313	3.6272	2.5608	4.0425	2.1120	2.4986	
F15	3.07E-04	3.07E-04	3.67E-03	1.65E-03	5.77E-04	2.22E-04	3.37E-04	6.25E-04	5.72E-04	3.24E-04
F16	-1.0316	7.49E-14	-1.0316	4.88E-16	-1.0316	6.25E-16	-1.0316	-1.0316	-1.0316	4.2E-07
F17	0.3979	3.09E-14	0.3979	0	0.3979	0	0.3979	0.3979	0.3979	2.7E-05
F18	3	1.70E-15	3	4.17E-15	3	1.33E-15	3	3	3	4.22E-15
F19	-3.8628	2.67E-15	-3.8628	2.29E-15	-3.8628	2.58E-15	-3.8626	-3.8628	-3.8562	0.0027
F20	-3.3220	2.69E-12	-3.3178	0.0231	-3.2663	0.0605	-3.2865	-3.2506	-2.9811	0.3767
F21	-10.1532	5.38E-11	-5.9551	3.7371	-6.8651	3.0196	-10.1514	-9.1402	-7.0492	3.6296
F22	-10.4029	1.14E-15	-9.6845	2.0141	-8.4565	3.0871	-10.4015	-8.5844	-8.1818	3.8292
F23	-10.5364	2.06E-15	-10.5364	2.6E-15	-9.9529	1.7828	-10.5343	-8.5590	-9.3424	2.4147

follows: $N_{PV} = 4000$, $I_{MPP} = 7.76\,A$, $V_{MPP} = 28.36\,V$, $I_{SC} = 8.38\,A$, $V_{oc} = 36.76\,V$, $K_i = 0.00545\,A/°C$, $K_v = 0.1278\,V/°C$, $T_A = 30.76°C$, and $N_{OT} = 43°C$ [47], [48]. Fig. 16 presents the hourly expected output of the PV module, defined based on Eqs. (34)-(42). The curve in Fig. 16 shows the hourly output of PV DGs as percentages of the daily peak outputs.

Table 8 shows the results of 33-bus and 69-bus RDNs considering daily variable load and PV DG uncertainty for a representative day. The results of ESGA are compared with the original SGA to validate its performance. Without PV DGs integration, 33-bus RDN has a total daily energy loss of 3420.3929 kW. After optimization, ESGA determines the optimal DG locations at buses 14, 24, and 30 with a total size of the DGs of 4.4409 MVA. Accordingly, the daily energy loss of the RDN is improved to 1689.1032 kW from 3420.3929 kW in the initial case (50.62 % reduction). Meanwhile, the optimal locations of three PV DGs are at bus 11, 21, and 61 with a total size of 3.9792 MVA for 69-bus RDN. Hence, energy loss is reduced to 1785.8079 kW (52.83 % reduction). From Table 8, ESGA also obtains better results than SGA for both case studies.

Fig. 17 shows the hourly power output of PV DGs of ESGA corresponding to the hourly load demands of the 33-bus and 69-bus RDNs, respectively. Fig. 18 illustrates the hourly power losses in the case of with and without DG integration for the 33-bus and 69-bus RDNs, respectively. As shown in Fig. 18, the output of PV DGs greatly reduces the power losses of the RDNs during the time span of 6 to 20 hours, a period when the load demand typically escalates.

Fig. 19 depicts the voltage profiles of the 33-bus and 69-bus RDNs for a representative day without DG integration, respectively. Meanwhile, the voltage profiles of two RDNs

with DG integration are presented in Fig. 20. During times when PV DGs generate power, the voltage profiles of both two RDNs are remarkably enhanced.

VI. CONCLUSION

This study effectively addressed the ODGP problem by formulating it with both single-objective and multi-objective functions. The first scenario considered active power loss as a single objective function. Meanwhile, three objective functions, namely active power loss minimization, voltage profile improvement, and voltage stability index maximization, were joined into a multi-objective problem using weighted coefficients. The ESGA was used to optimize the distribution of DGs in RDNs, meeting all operating constraints. Simulation tests were conducted on three RDNs of different sizes, with DG units considered at two power factors. The results indicated that the optimal DG power factors pointedly decreased active power losses, enhanced voltage deviation, and boosted the voltage stability index. The ESGA outperformed other methods in terms of solution quality, accuracy, and convergence speed, especially for large-scale systems. Therefore, ESGA is a highly recommended approach for solving the ODGP problem.

APPENDIX

To assess the algorithm's performance, ESGA is evaluated using the 23 benchmark functions labeled as F1 - F23. Detailed definitions of these issues are taken from [49], [50], and [51]. Despite the simplicity, numerous researchers have employed these test functions to verify their proposed methods. The simulations are conducted with a population size of 30 and maximum iterations of 500. The best results obtained by ESGA over 30 independent runs are collected and

compared with published results in [49], [50], including GSA, PSO, grey wolf optimization (GWO), and whale optimizer algorithm (WOA).

Table 9 presents the statistical results of ESGA and other methods for 23 benchmark functions. Out of a total of 23 test functions, ESGA achieves similar results with other algorithms for 4 functions (i.e., F16, F17, F18, and F19) and surpasses other algorithms for 11 functions (i.e., F5, F8, F11-F15, and F20-F23). Meanwhile, the results obtained from ESGA are very competitive for the remaining functions. The good performance of ESGA for these test functions indicates that ESGA strikes an effective balance between exploitation and exploration, leading to a strong ability to avoid local optima.

REFERENCES

[1] K. H. Truong, P. Nallagownden, I. Elamvazuthi, and D. N. Vo, "A quasi-oppositional-chaotic symbiotic organisms search algorithm for optimal allocation of DG in radial distribution networks," *Appl. Soft Comput.*, vol. 88, Mar. 2020, Art. no. 106067.

[2] *Global Electricity Demand to Increase 57% by 2050 | BloombergNEF*. Accessed: Aug. 20, 2023. [Online]. Available: https://about.bnef.com/blog/global-electricity-demand-increase-57-2050/

[3] P. Paliwal, N. P. Patidar, and R. K. Nema, "Planning of grid integrated distributed generators: A review of technology, objectives and techniques," *Renew. Sustain. Energy Rev.*, vol. 40, pp. 557–570, Dec. 2014.

[4] T. H. B. Huy, T. V. Tran, D. N. Vo, and H. T. T. Nguyen, "An improved metaheuristic method for simultaneous network reconfiguration and distributed generation allocation," *Alexandria Eng. J.*, vol. 61, no. 10, pp. 8069–8088, Oct. 2022.

[5] N. Acharya, P. Mahat, and N. Mithulananthan, "An analytical approach for DG allocation in primary distribution network," *Int. J. Electr. Power Energy Syst.*, vol. 28, no. 10, pp. 669–678, Dec. 2006.

[6] D. Q. Hung, N. Mithulananthan, and R. C. Bansal, "Analytical expressions for DG allocation in primary distribution networks," *IEEE Trans. Energy Convers.*, vol. 25, no. 3, pp. 814–820, Sep. 2010.

[7] P. Kayal, S. Chanda, and C. K. Chanda, "An analytical approach for allocation and sizing of distributed generations in radial distribution network," *Int. Trans. Electr. Energy Syst.*, vol. 27, no. 7, p. e2322, Jul. 2017.

[8] M. F. Shaaban, Y. M. Atwa, and E. F. El-Saadany, "DG allocation for benefit maximization in distribution networks," *IEEE Trans. Power Syst.*, vol. 28, no. 2, pp. 639–649, May 2013.

[9] C. Wu, Y. Lou, P. Lou, and H. Xiao, "DG location and capacity optimization considering several objectives with cloud theory adapted GA," *Int. Trans. Electr. Energy Syst.*, vol. 24, no. 8, pp. 1076–1088, Aug. 2014.

[10] S. Ganguly and D. Samajpati, "Distributed generation allocation with on-load tap changer on radial distribution networks using adaptive genetic algorithm," *Appl. Soft Comput.*, vol. 59, pp. 45–67, Oct. 2017.

[11] A. M. El-Zonkoly, "Optimal placement of multi-distributed generation units including different load models using particle swarm optimization," *Swarm Evol. Comput.*, vol. 1, no. 1, pp. 50–59, Mar. 2011.

[12] S. Kansal, V. Kumar, and B. Tyagi, "Optimal placement of different type of DG sources in distribution networks," *Int. J. Electr. Power Energy Syst.*, vol. 53, pp. 752–760, Dec. 2013.

[13] R. S. Maciel, M. Rosa, V. Miranda, and A. Padilha-Feltrin, "Multi-objective evolutionary particle swarm optimization in the assessment of the impact of distributed generation," *Electr. Power Syst. Res.*, vol. 89, pp. 100–108, Aug. 2012.

[14] A. Soroudi and M. Afrasiab, "Binary PSO-based dynamic multi-objective model for distributed generation planning under uncertainty," *IET Renew. Power Gener.*, vol. 6, pp. 67–78, Mar. 2012.

[15] M. Gomez-Gonzalez, A. López, and F. Jurado, "Optimization of distributed generation systems using a new discrete PSO and OPF," *Electr. Power Syst. Res.*, vol. 84, no. 1, pp. 174–180, Mar. 2012.

[16] I. A. Quadri, S. Bhowmick, and D. Joshi, "A comprehensive technique for optimal allocation of distributed energy resources in radial distribution systems," *Appl. Energy*, vol. 211, pp. 1245–1260, Feb. 2018.

[17] F. S. Abu-Mouti and M. E. El-Hawary, "Optimal distributed generation allocation and sizing in distribution systems via artificial bee colony algorithm," *IEEE Trans. Power Del.*, vol. 26, no. 4, pp. 2090–2101, Oct. 2011.

[18] Z. Moravej and A. Akhlaghi, "A novel approach based on cuckoo search for DG allocation in distribution network," *Int. J. Electr. Power Energy Syst.*, vol. 44, no. 1, pp. 672–679, Jan. 2013.

[19] A. El-Fergany, "Optimal allocation of multi-type distributed generators using backtracking search optimization algorithm," *Int. J. Electr. Power Energy Syst.*, vol. 64, pp. 1197–1205, Jan. 2015.

[20] E. S. Ali, S. M. A. Elazim, and A. Y. Abdelaziz, "Ant lion optimization algorithm for renewable distributed generations," *Energy*, vol. 116, pp. 445–458, Dec. 2016.

[21] S. Sultana and P. K. Roy, "Krill herd algorithm for optimal location of distributed generator in radial distribution system," *Appl. Soft Comput.*, vol. 40, pp. 391–404, Mar. 2016.

[22] A. Fathy, D. Yousri, H. Rezk, and H. S. Ramadan, "An efficient capuchin search algorithm for allocating the renewable based biomass distributed generators in radial distribution network," *Sustain. Energy Technol. Assessments*, vol. 53, Oct. 2022, Art. no. 102559.

[23] A. Fathy, D. Yousri, A. Y. Abdelaziz, and H. S. Ramadan, "Robust approach based chimp optimization algorithm for minimizing power loss of electrical distribution networks via allocating distributed generators," *Sustain. Energy Technol. Assessments*, vol. 47, Oct. 2021, Art. no. 101359.

[24] M. H. Ali, S. Kamel, M. H. Hassan, M. Tostado-Véliz, and H. M. Zawbaa, "An improved wild horse optimization algorithm for reliability based optimal DG planning of radial distribution networks," *Energy Rep.*, vol. 8, pp. 582–604, Nov. 2022.

[25] J. Qian, P. Wang, C. Pu, X. Peng, and G. Chen, "Application of effective gravitational search algorithm with constraint priority and expert experience in optimal allocation problems of distribution network," *Eng. Appl. Artif. Intell.*, vol. 117, Jan. 2023, Art. no. 105533.

[26] A. Fathy, "A novel artificial hummingbird algorithm for integrating renewable based biomass distributed generators in radial distribution systems," *Appl. Energy*, vol. 323, Oct. 2022, Art. no. 119605.

[27] T. T. Nguyen, T. T. Nguyen, and M. Q. Duong, "An improved equilibrium optimizer for optimal placement of photovoltaic systems in radial distribution power networks," *Neural Comput. Appl.*, vol. 34, no. 8, pp. 6119–6148, Apr. 2022.

[28] L. D. L. Nguyen, P. K. Nguyen, V. C. Vo, N. D. Vo, T. T. Nguyen, and T. M. Phan, "Applications of recent metaheuristic algorithms for loss reduction in distribution power systems considering maximum penetration of photovoltaic units," *Int. Trans. Electr. Energy Syst.*, vol. 2023, pp. 1–23, Mar. 2023.

[29] M. H. Moradi and M. Abedini, "A combination of genetic algorithm and particle swarm optimization for optimal DG location and sizing in distribution systems," *Int. J. Electr. Power Energy Syst.*, vol. 34, no. 1, pp. 66–74, Jan. 2012.

[30] M. H. Moradi and M. Abedini, "A novel method for optimal DG units capacity and location in microgrids," *Int. J. Electr. Power Energy Syst.*, vol. 75, pp. 236–244, Feb. 2016.

[31] S. Kansal, V. Kumar, and B. Tyagi, "Hybrid approach for optimal placement of multiple DGs of multiple types in distribution networks," *Int. J. Electr. Power Energy Syst.*, vol. 75, pp. 226–235, Feb. 2016.

[32] K. Mahmoud, N. Yorino, and A. Ahmed, "Optimal distributed generation allocation in distribution systems for loss minimization," *IEEE Trans. Power Syst.*, vol. 31, no. 2, pp. 960–969, Mar. 2016.

[33] T. P. Nguyen and D. N. Vo, "A novel stochastic fractal search algorithm for optimal allocation of distributed generators in radial distribution systems," *Appl. Soft Comput.*, vol. 70, pp. 773–796, Sep. 2018.

[34] S. Saha and V. Mukherjee, "Optimal placement and sizing of DGs in RDS using chaos embedded SOS algorithm," *IET Gener., Transmiss. Distrib.*, vol. 10, no. 14, pp. 3671–3680, Nov. 2016.

[35] S. Sharma, S. Bhattacharjee, and A. Bhattacharya, "Quasi-oppositional swine influenza model based optimization with quarantine for optimal allocation of DG in radial distribution network," *Int. J. Electr. Power Energy Syst.*, vol. 74, pp. 348–373, Jan. 2016.

[36] S. Sultana and P. K. Roy, "Multi-objective quasi-oppositional teaching learning based optimization for optimal location of distributed generator in radial distribution systems," *Int. J. Electr. Power Energy Syst.*, vol. 63, pp. 534–545, Dec. 2014.

[37] *IEEE Standard for Interconnection and Interoperability of Distributed Energy Resources With Associated Electric Power Systems Interfaces*, IEEE Standard 1547-2018, 2018, pp. 1–138.

[38] M. Chakravorty and D. Das, "Voltage stability analysis of radial distribution networks," *Int. J. Electr. Power Energy Syst.*, vol. 23, no. 2, pp. 129–135, Feb. 2001.

[39] M. S. Gonçalves, R. H. Lopez, and L. F. F. Miguel, "Search group algorithm: A new metaheuristic method for the optimization of truss structures," *Comput. Struct.*, vol. 153, pp. 165–184, Jun. 2015.

[40] J. Ji, S. Gao, S. Wang, Y. Tang, H. Yu, and Y. Todo, "Self-adaptive gravitational search algorithm with a modified chaotic local search," *IEEE Access*, vol. 5, pp. 17881–17895, 2017.

[41] D. Jia, G. Zheng, and M. K. Khan, "An effective memetic differential evolution algorithm based on chaotic local search," *Inf. Sci.*, vol. 181, no. 15, pp. 3175–3187, Aug. 2011.

[42] R. D. Zimmerman and C. E. Murillo-Sanchez, "Matpower 6.0 user's manual," Cornell Univ., Ithaca, NY, USA. Accessed: Aug. 20, 2023. [Online]. Available: https://matpower.org/docs/MATPOWER-manual-6.0.pdf

[43] M. E. Baran and F. F. Wu, "Network reconfiguration in distribution systems for loss reduction and load balancing," *IEEE Trans. Power Del.*, vol. 4, no. 2, pp. 1401–1407, Apr. 1989.

[44] M. E. Baran and F. F. Wu, "Optimal capacitor placement on radial distribution systems," *IEEE Trans. Power Del.*, vol. 4, no. 1, pp. 725–734, Jan. 1989.

[45] D. Zhang, Z. Fu, and L. Zhang, "An improved TS algorithm for loss-minimum reconfiguration in large-scale distribution systems," *Electr. Power Syst. Res.*, vol. 77, nos. 5–6, pp. 685–694, Apr. 2007.

[46] D. Q. Hung, N. Mithulananthan, and R. C. Bansal, "Analytical strategies for renewable distributed generation integration considering energy loss minimization," *Appl. Energy*, vol. 105, pp. 75–85, May 2013.

[47] D. Q. Hung, N. Mithulananthan, and R. C. Bansal, "Integration of PV and BES units in commercial distribution systems considering energy loss and voltage stability," *Appl. Energy*, vol. 113, pp. 1162–1170, Jan. 2014.

[48] D. Q. Hung, N. Mithulananthan, and K. Y. Lee, "Determining PV penetration for distribution systems with time-varying load models," *IEEE Trans. Power Syst.*, vol. 29, no. 6, pp. 3048–3057, Nov. 2014.

[49] S. Mirjalili, S. M. Mirjalili, and A. Lewis, "Grey wolf optimizer," *Adv. Eng. Softw.*, vol. 69, pp. 46–61, Mar. 2014.

[50] S. Mirjalili and A. Lewis, "The whale optimization algorithm," *Adv. Eng. Softw.*, vol. 95, pp. 51–67, May 2016.

[51] S. Mirjalili, "Moth-flame optimization algorithm: A novel nature-inspired heuristic paradigm," *Knowl.-Based Syst.*, vol. 89, pp. 228–249, Nov. 2015.

DIEU NGOC VO received the B.Eng. and M.Eng. degrees in electrical engineering from the Ho Chi Minh City University of Technology (HCMUT), VNU-HCM, Ho Chi Minh City, Vietnam, in 1995 and 2000, respectively, and the D.Eng. degree in energy from the Asian Institute of Technology (AIT), Pathum Thani, Thailand, in 2007. He is currently an Associate Professor with the Department of Power Systems, Faculty of Electrical and Electronic Engineering, HCMUT, VNU-HCM. His research interests include applications of AI in power system optimization, power system operation and control, power system analysis, and power systems under deregulation.

KHOA HOANG TRUONG received the B.Eng. degree in electrical engineering from the Ho Chi Minh City University of Technology, VNU-HCM, Vietnam, in 2012, and the M.Sc. and Ph.D. degrees in electrical and electronic engineering from Universiti Teknologi Petronas (UTP), Malaysia, in 2016 and 2020, respectively. He is currently a Lecturer with the Department of Power Delivery, Faculty of Electrical and Electronic Engineering, HCMUT. His research interests include power system operation and control, distributed generation, artificial intelligence-based algorithms, and their application in power system optimization problems.

TRUONG HOANG BAO HUY received the B.Eng. degree in electrical and electronics engineering from the Ho Chi Minh City University of Technology (HCMUT), VNU-HCM, Vietnam, in 2017, and the M.S. degree in electrical and electronics engineering from Universiti Teknologi Petronas (UTP), Malaysia, in 2020. He is currently pursuing the Ph.D. degree with the Department of Future Convergence Technology, Soonchunhyang University, Asan-si, South Korea. His research interests include energy management, smart grids, microgrids, and artificial intelligence-based algorithms and their application in optimization problems.

THANH VAN TRAN received the B.Eng., M.Eng., and D.Eng. degrees in electrical engineering from the Kyiv Polytechnic Institute, Kyiv, Ukraine, in 1992, 1994, and 2000, respectively. He is currently a Senior Lecturer with the Institute of Engineering and Technology, Thu Dau Mot University, Binh Duong, Vietnam. His research interests include applications of AI in power system optimization, power system operation and control, and power system analysis.

• • •